Transverse wavevector dependent and frequency dependent dielectric function, magnetic permittivity and generalized conductivity of interaction site fluids. MD calculations for the TIP4P water

Igor P. Omelyan

Institute for Condensed Matter Physics, the National Ukrainian Academy of Sciences, 1 Svientsitsky St., UA-290011 Lviv, Ukraine *

Abstract

It is shown that the dielectric properties of interaction site models of polar fluids can be investigated in computer experiment using not only the charge fluctuations but also correlations corresponding to a current of moving charges. This current can be associated with a generalized dynamical polarization or separated into electric and magnetic components. The first approach deals with the dielectric permittivity related to a generalized conductivity, whereas the second one leads to the functions describing polarization and magnetization fluctuations separately. The last way is only the source to calculate the magnetic susceptibility for a system of interaction sites. The transverse wavevector- and frequency-dependent dielectric functions and magnetic susceptibility are evaluated for the TIP4P water model in a very wide scale of wavelengths and frequencies using molecular dynamics simulations. We demonstrate that the transverse part of the dielectric functions may differ drastically from their longitudinal component. A relationship between the two approaches is discussed and the limiting transition to the static dielectric constant in the infinite-wavelength regime is analyzed. The propagation of transverse electromagnetic waves in the TIP4P water is also considered.

*E-mail: nep@icmp.lviv.ua

I. MOTIVATION

In a recent paper [1], a computer adapted fluctuation formula suitable for self-consistent calculations of the longitudinal wavevector- and frequency-dependent dielectric function $\varepsilon_{\rm L}(k,\omega)$ for interaction site models (ISMs) of polar systems has been proposed. As a result, a detailed analysis of this function in the entire wavelength and time scales was carried out for the TIP4P water model using molecular dynamics (MD). It was shown that the choice of microscopic variables for the operator $\hat{\boldsymbol{P}}$ of polarization density plays an important role in a correct reproduction of dielectric properties, and only true microscopic variables, which explicitly take into account the charge distribution within molecules, can be used to determine the frequency dependence of the dielectric permittivity of ISMs at arbitrary wavenumbers.

It is a common practice to investigate the dielectric properties of ISMs on the basis of charge fluctuations [1–3]. In the infinite-wavelength limit $k \to 0$, these fluctuations reduce to the well-known longitudinal dipole moment correlations, which are usually considered in computer experiment to obtain $\varepsilon_{\rm L}(k,\omega)$ at zero and small wavevector values [4–12]. The transverse dipole moment fluctuations are used sometimes [5, 9, 10–12] for treating the transverse component $\varepsilon_{\rm T}(k,\omega)$ of the dielectric permittivity. However, such an approach, being exact for point dipole systems [13, 14], cannot be applied to calculations of the genuine transverse dielectric function of ISMs at nonzero wavenumbers.

The problem of computations of $\varepsilon_{\rm T}(k,\omega)$ for ISM fluids is due to difficulties [15, 16] when constructing the transverse part of $\hat{\boldsymbol{P}}$. While the longitudinal part $\hat{\boldsymbol{P}}_{\rm L}$ can easily be expressed in terms of the operator of charge density, to define the transverse component $\hat{\boldsymbol{P}}_{\rm T}$ involving additional dynamical variables is necessary. There are two approaches for describing the electromagnetic phenomena in ISMs. They differ between themselves in the way of how to treat the current of moving charges. In the abbreviated approach [17], electric and magnetic parts of the total current are undistinguishable from one another in the presence of spatially inhomogeneous fields, i.e, when $k \neq 0$. In such a case, the magnetic part is included into a generalized $\hat{\boldsymbol{P}}$-vector and the electromagnetic phenomena in the system are determined by a transverse dielectric permittivity $\varepsilon_{\rm T}(k,\omega)$ which is directly connected with the generalized conductivity $\sigma_{\rm T}(k,\omega) = \frac{{\rm i}\omega}{4\pi}(\varepsilon_{\rm T}(k,\omega)-1)$. The second approach [18] is based on a separation of the microscopic current into electric and magnetic parts at arbitrary wavenumbers. This leads to the introduction of two functions, $\epsilon_{\rm T}(k,\omega) \neq \varepsilon_{\rm T}(k,\omega)$ and $\mu(k,\omega)$, describing the transverse fluctuations

of polarization and magnetization densities separately. The last function is associated with a generalized magnetic permittivity of ISM systems. In this approach the transverse dielectric permittivity $\varepsilon_{\rm T}(k,\omega)$ can easily be reproduced using functions $\epsilon_{\rm T}(k,\omega)$ and $\mu(k,\omega)$. In the infinite-wavelength limit $k \to 0$, when the spatial dispersion can be neglected, the two approaches become completely equivalent. In this case the electric phenomena are uniquely described by the frequency-dependent dielectric constant $\varepsilon(\omega) = \lim_{k\to 0} \epsilon_{\rm T}(k,\omega) = \lim_{k\to 0} \varepsilon_{\rm L,T}(k,\omega)$, whereas a magnetic state is determined by the magnetic permittivity $\mu(\omega) = \lim_{k\to 0} \mu(k,\omega) = [1 - \frac{\omega^2}{c^2} \lim_{k\to 0}(\varepsilon_{\rm T}(k,\omega) - \varepsilon_{\rm L}(k,\omega))/k^2]^{-1}$, where c denotes the velocity of light [17].

Until recently, quite a few papers [19, 20] dealt with the investigation of correlations related to the current of charges in ISMs. In these articles, spectra of the longitudinal and transverse components of the hydrogen current, on the time scale peculiar to the librational dynamics of water, were calculated for the TIP4P potential at small wavenumbers. The first calculation of the transverse dielectric function $\epsilon_{\rm T}(k) = \lim_{\omega\to 0} \epsilon_{\rm T}(k,\omega)$ has been performed by Raineri and Friedman [16], but in the static regime only and for the simplest ξDS model. At the same time, there were no attempts to investigate the entire wavevector and frequency dependence of the transverse dielectric function and the magnetic susceptibility for ISM fluids.

In the present paper the dielectric properties of ISMs are investigated on the basis of current correlations, including their separation into electric and magnetic parts. This allows us to determine both the longitudinal and transverse components of the dielectric permittivity $\varepsilon(k,\omega)$ as well as the dielectric $\epsilon_{\rm T}(k,\omega)$ and magnetic $\mu(k,\omega)$ functions. Actual MD simulations are performed for the TIP4P model of water using the interaction site reaction field (ISRF) geometry [3] and the Ewald method. The results obtained for $\epsilon_{\rm T}(k,\omega)$ and $\mu(k,\omega)$ are presented in a wide region of wavevectors and frequencies.

II. ELECTROMAGNETIC FLUCTUATION FORMULAS FOR ISM FLUIDS

A. Generalized dielectric constant and conductivity

We shall consider a polar fluid consisting of N identical molecules which are composed of M interaction sites and enclosed in a volume V. The microscopic density of charges for such a system at point $\boldsymbol{r} \in V$ and time t is of the form $\hat{Q}(\boldsymbol{r},t) = \sum_{i=1}^{N} \sum_{a=1}^{M} q_a \delta(\boldsymbol{r} - \boldsymbol{r}_i^a(t))$, where q_a and $\boldsymbol{r}_i^a(t)$ are the charge and position of site a within molecule i, respectively.

Shifting from the real coordinate space $\{\boldsymbol{r}\}$ into the $\{\boldsymbol{k}\}$-representation by the spatial Fourier transform $\{\boldsymbol{k}\} = \int_V \{\boldsymbol{r}\} \mathrm{e}^{-\mathrm{i}\boldsymbol{k}\cdot\boldsymbol{r}} \mathrm{d}\boldsymbol{r}$, we obtain that $\hat{Q}(\boldsymbol{k},t) = \sum_{i=1}^{N}\sum_{a=1}^{M} q_a \mathrm{e}^{-\mathrm{i}\boldsymbol{k}\cdot\boldsymbol{r}_i^a(t)}$. For the investigation of dielectric properties, it is convenient to introduce the microscopic vector $\hat{\boldsymbol{P}}(\boldsymbol{k},t)$ of polarization density. The longitudinal part $\hat{\boldsymbol{P}}_{\mathrm{L}} = \hat{\boldsymbol{k}}\,\hat{\boldsymbol{P}}\cdot\hat{\boldsymbol{k}}$ of this vector can be determined using the relation $\hat{Q}(\boldsymbol{r},t) = -\mathrm{div}\hat{\boldsymbol{P}}(\boldsymbol{r},t)$ in $\boldsymbol{k}$-space, i.e., $\hat{Q}(\boldsymbol{k},t) = -\mathrm{i}\boldsymbol{k}\cdot\hat{\boldsymbol{P}}(\boldsymbol{k},t)$. Then we find

$$\hat{\boldsymbol{P}}_{\mathrm{L}}(\boldsymbol{k},t) = \frac{\mathrm{i}\boldsymbol{k}}{k^2}\hat{Q}(\boldsymbol{k},t) = \frac{\mathrm{i}\hat{\boldsymbol{k}}}{k}\sum_{i=1}^{N}\sum_{a=1}^{M} q_a \mathrm{e}^{-\mathrm{i}\boldsymbol{k}\cdot\boldsymbol{r}_i^a(t)} \ , \tag{1}$$

where $\hat{\boldsymbol{k}} = \boldsymbol{k}/k$ is the unit vector directed along $\boldsymbol{k}$.

Recently [1], it has been shown that the longitudinal component $\varepsilon_{\mathrm{L}}(k,\omega)$ of the wavevector- and frequency-dependent dielectric tensor can be calculated in computer experiment via the fluctuation formula

$$\frac{\varepsilon_{\mathrm{L}}(k,\omega)-1}{\varepsilon_{\mathrm{L}}(k,\omega)} = \frac{h\mathscr{L}_{\mathrm{i}\omega}(-\dot{G}_{\mathrm{L}}(k,t))}{1+hD(k)\mathscr{L}_{\mathrm{i}\omega}(-\dot{G}_{\mathrm{L}}(k,t))} = h\mathscr{L}_{\mathrm{i}\omega}(-\dot{g}_{\mathrm{L}}(k,t)) \ . \tag{2}$$

Here, $G_{\mathrm{L}}(k,t) = \left\langle \hat{\boldsymbol{P}}_{\mathrm{L}}(\boldsymbol{k},0)\cdot\hat{\boldsymbol{P}}_{\mathrm{L}}(-\boldsymbol{k},t)\right\rangle_0 \Big/ Nd^2$ is the longitudinal wavevector-dependent dynamical Kirkwood factor computed in simulation for a finite sample, $\langle\ \rangle_0$ denotes the statistical averaging in the absence of external fields, d designates the permanent magnitude of molecule's dipole moment $\boldsymbol{d}_i = \sum_a^M q_a \boldsymbol{r}_i^a$, the Laplace transform is defined as $\mathscr{L}_{\mathrm{i}\omega}(\{t\}) = \int_0^\infty \{t\}\ \mathrm{e}^{-\mathrm{i}\omega t}\mathrm{d}t$, k_{B} and T are the Boltzmann's constant and the temperature of the system, respectively, $h = 4\pi N d^2 \big/ V k_{\mathrm{B}} T$ and $\dot{G}_{\mathrm{L}}(k,t) \equiv \partial G_{\mathrm{L}}(k,t)/\partial t$. The function $D(k)$ takes into account boundary conditions, applied in simulation, and for finite samples it always is equal to 1 at $k = 0$. For nonzero wavevectors this function tends to zero in the case of Ewald summation, while $D(k) = 3j_1(kR)/(kR)$ within the reaction field geometry [1, 3], where R and $j_1(z) = \sin(z)/z^2 - \cos(z)/z$ are the cut-off radius and spherical Bessel function of first order, respectively. For infinite systems ($R \to \infty$) the function $D(k)$ is equal to zero at arbitrary wavenumbers and the computer adapted formula (2) reduces to the well-known fluctuation formula in terms of the infinite-system Kirkwood factor $g_{\mathrm{L}}(k,t) = \lim_{N\to\infty} G_{\mathrm{L}}(k,t)$.

As we can see, using the microscopic operator $\hat{Q}(\boldsymbol{k},t)$ of charge density allows one to determine uniquely only the longitudinal part of polarization vector $\hat{\boldsymbol{P}}(\boldsymbol{k},t)$. To construct the transverse part, it is necessary to involve additional dynamical variables. We shall show now how to derive fluctuation formulas which give the possibility to computer both the longitudinal as well as the transverse component of the dielectric constant of ISMs.

The processes of dynamical polarization in dielectrics cause a current of charges. This current is described by the microscopic operator of current density $\hat{\boldsymbol{I}}$ and may be associated with the generalized polarization current [17], so that

$$\hat{\boldsymbol{I}}(\boldsymbol{k},t)=\sum_{i,a}^{N,M} q_a \boldsymbol{V}_i^a(t)\mathrm{e}^{-\mathrm{i}\boldsymbol{k}\cdot\boldsymbol{r}_i^a(t)}=\frac{\mathrm{d}}{\mathrm{d}t}\hat{\boldsymbol{P}}(\boldsymbol{k},t)\ , \tag{3}$$

where $\boldsymbol{V}_i^a(t)$ denotes the velocity of site a within the molecule i at time t. The relation (3) can be considered as a more general definition of $\hat{\boldsymbol{P}}$-vector, because it allows to determine its longitudinal $\hat{\boldsymbol{P}}_{\mathrm{L}}=\hat{\boldsymbol{k}}\,\hat{\boldsymbol{P}}\cdot\hat{\boldsymbol{k}}$ and transverse $\hat{\boldsymbol{P}}_{\mathrm{T}}=(\mathbf{1}-\hat{\boldsymbol{k}}\hat{\boldsymbol{k}})\hat{\boldsymbol{P}}=\hat{\boldsymbol{k}}\times[\hat{\boldsymbol{P}}\times\hat{\boldsymbol{k}}]$ components, where $\mathbf{1}$ is the unit tensor of the second rank. It is worth to emphasize that the generalized vector $\hat{\boldsymbol{P}}$ of polarization induction includes both electric as well as magnetic contributions (see a more detailed discussion of this point in the next subsection). In a particular case of longitudinal polarization this vector satisfies completely our previous definition (1) of $\hat{\boldsymbol{P}}_{\mathrm{L}}$. Indeed, taking the full derivative of (1) with respect to time, it can be verified easily on the basis of equation (3) that $\frac{\mathrm{d}}{\mathrm{d}t}\hat{\boldsymbol{P}}_{\mathrm{L}}(\boldsymbol{k},t)=\hat{\boldsymbol{k}}\,\hat{\boldsymbol{k}}\cdot\hat{\boldsymbol{I}}(\boldsymbol{k},t)\equiv\hat{\boldsymbol{I}}_{\mathrm{L}}(\boldsymbol{k},t)$.

Let us apply to the system under consideration an external electric field $\boldsymbol{E}_0(\boldsymbol{k},t)$ which contains longitudinal $\boldsymbol{E}_0^{\mathrm{L}}$ and transverse $\boldsymbol{E}_0^{\mathrm{T}}$ components. The total field in the system $\hat{\boldsymbol{E}}(\boldsymbol{k},t)$ consists of the external field and an internal field of charged sites. Neglecting the relativistic terms due to the dynamical magnetic field of moving charges, the internal field can be presented [1, 3] in the purely longitudinal form $-4\pi(1-D(k))\hat{\boldsymbol{P}}_{\mathrm{L}}$. Therefore, the longitudinal and transverse components of the total field $\hat{\boldsymbol{E}}=\hat{\boldsymbol{E}}_{\mathrm{L}}+\hat{\boldsymbol{E}}_{\mathrm{T}}$ are equal to $\hat{\boldsymbol{E}}_{\mathrm{L}}(\boldsymbol{k},t)=\boldsymbol{E}_0^{\mathrm{L}}(\boldsymbol{k},t)-4\pi(1-D(k))\hat{\boldsymbol{P}}_{\mathrm{L}}(\boldsymbol{k},t)$ and $\hat{\boldsymbol{E}}_{\mathrm{T}}(\boldsymbol{k},t)=\boldsymbol{E}_0^{\mathrm{T}}(\boldsymbol{k},t)$, respectively. The longitudinal $\varepsilon_{\mathrm{L}}(k,\omega)$ and transverse $\varepsilon_{\mathrm{T}}(k,\omega)$ components of the wavevector- and frequency-dependent dielectric tensor $\boldsymbol{\varepsilon}(\boldsymbol{k},\omega)=\varepsilon_{\mathrm{T}}(k,\omega)\mathbf{1}+(\varepsilon_{\mathrm{L}}(k,\omega)-\varepsilon_{\mathrm{T}}(k,\omega))\hat{\boldsymbol{k}}\hat{\boldsymbol{k}}$ can be defined via the material relations $\boldsymbol{P}_{\mathrm{L,T}}(\boldsymbol{k},\omega)=\frac{1}{4\pi}(\varepsilon_{\mathrm{L,T}}(k,\omega)-1)\ \boldsymbol{E}_{\mathrm{L,T}}(\boldsymbol{k},\omega)$, where $\boldsymbol{P}_{\mathrm{L,T}}(\boldsymbol{k},\omega)=\left\langle\hat{\boldsymbol{P}}_{\mathrm{L,T}}(\boldsymbol{k},\omega)\right\rangle$ and $\boldsymbol{E}_{\mathrm{L,T}}(\boldsymbol{k},\omega)=\left\langle\hat{\boldsymbol{E}}_{\mathrm{L,T}}(\boldsymbol{k},\omega)\right\rangle$ are macroscopic values of the polarization and total field, $\langle\ \rangle$ denotes the statistical averaging in the presence of the external field and the time Fourier transform $\{\omega\}=\int_{-\infty}^{\infty}\{t\}\mathrm{e}^{-\mathrm{i}\omega t}\mathrm{d}t$ has been used for functions $\hat{\boldsymbol{P}}_{\mathrm{L,T}}(\boldsymbol{k},t)$ and $\hat{\boldsymbol{E}}_{\mathrm{L,T}}(\boldsymbol{k},t)$.

In the case of dynamical polarization, when $\boldsymbol{I}(\boldsymbol{k},\omega)=\left\langle\hat{\boldsymbol{I}}(\boldsymbol{k},\omega)\right\rangle\neq 0$ at $\omega\neq 0$ (note that static macroscopic currents of coupled charges are equal to zero), the Maxwell equations can be written in a form as for conductors, namely, in terms of the generalized polarization conductivity $\sigma(k,\omega)$. The longitudinal and transverse components $\sigma_{\mathrm{L,T}}(k,\omega)$ of this wavevector- and frequency-dependent conductivity are defined via the material relations $\boldsymbol{I}_{\mathrm{L,T}}(\boldsymbol{k},\omega)=\sigma_{\mathrm{L,T}}(k,\omega)\boldsymbol{E}_{\mathrm{L,T}}(\boldsymbol{k},\omega)$. In the frequency representation, equation

(3) stays that $\hat{\boldsymbol{I}}_{\mathrm{L,T}}(\boldsymbol{k},\omega) = \mathrm{i}\omega\hat{\boldsymbol{P}}_{\mathrm{L,T}}(\boldsymbol{k},\omega)$. Thus we can express the dielectric constant in terms of the polarization conductivity as follows

$$\varepsilon_{\mathrm{L,T}}(k,\omega) - 1 = \frac{4\pi\sigma_{\mathrm{L,T}}(k,\omega)}{\mathrm{i}\omega} \ . \tag{4}$$

According to the perturbation theory of first order with respect to external fields, we obtain for the macroscopic current $\boldsymbol{I}_{\mathrm{L,T}}(\boldsymbol{k},\omega) = \mathscr{L}_{\mathrm{i}\omega}\left\langle \hat{\boldsymbol{I}}_{\mathrm{L,T}}(\boldsymbol{k},0)\cdot\hat{\boldsymbol{I}}_{\mathrm{L,T}}(-\boldsymbol{k},t)\right\rangle_0 \frac{\boldsymbol{E}_0^{\mathrm{L,T}}(\boldsymbol{k},\omega)}{\{2\}Vk_{\mathrm{B}}T}$, where the multiplier $\{2\}$ is to be included for the transverse component only. Then eliminating the electric fields and using relation (4) yields

$$\frac{\varepsilon_{\mathrm{L}}(k,\omega)-1}{\varepsilon_{\mathrm{L}}(k,\omega)} = \frac{h\mathscr{L}_{\mathrm{i}\omega}(C_{\mathrm{L}}(k,t))}{\mathrm{i}\omega + hD(k)\mathscr{L}_{\mathrm{i}\omega}(C_{\mathrm{L}}(k,t))} = \frac{h}{\mathrm{i}\omega}\mathscr{L}_{\mathrm{i}\omega}(c_{\mathrm{L}}(k,t)) \ , \tag{5}$$

$$\varepsilon_{\mathrm{T}}(k,\omega) - 1 = \frac{h}{\mathrm{i}\omega}\mathscr{L}_{\mathrm{i}\omega}(c_{\mathrm{T}}(k,t)) \ , \tag{6}$$

where

$$C_{\mathrm{L,T}}(k,t) = \frac{\left\langle \hat{\boldsymbol{I}}_{\mathrm{L,T}}(\boldsymbol{k},0)\cdot\hat{\boldsymbol{I}}_{\mathrm{L,T}}(-\boldsymbol{k},t)\right\rangle_0}{\{2\}Nd^2} \tag{7}$$

are the longitudinal and transverse components of the wavevector-dependent dynamical Kirkwood factor of second order for the finite sample, whereas $c_{\mathrm{L,T}}(k,t)$ are the corresponding functions of the infinite system and $c_{\mathrm{T}}(k,t) = C_{\mathrm{T}}(k,t)$.

The fluctuation formulas (5) and (6) can be used in simulations to evaluate the longitudinal and transverse components of the dielectric constant on the basis of equilibrium current-current correlations (7). In the case of longitudinal fluctuations, the formula (5) is mathematically equivalent to the usual relation (2). Indeed, in view of the equality $\hat{\boldsymbol{I}}_{\mathrm{L}}(\boldsymbol{k},t) = \frac{\mathrm{d}}{\mathrm{d}t}\hat{\boldsymbol{P}}_{\mathrm{L}}(\boldsymbol{k},t)$, it can be shown easily that $C_{\mathrm{L}}(k,t) = -\frac{\partial^2}{\partial t^2}G_{\mathrm{L}}(k,t) \equiv -\ddot{G}_{\mathrm{L}}(k,t)$. Then applying the Laplace transform we obtain $\mathscr{L}_{\mathrm{i}\omega}(C_{\mathrm{L}}(k,t)) = \dot{G}_{\mathrm{L}}(k,0) + \mathrm{i}\omega\mathscr{L}_{\mathrm{i}\omega}(-\dot{G}_{\mathrm{L}}(k,t))$, where $\dot{G}_{\mathrm{L}}(k,0) = 0$ because the Kirkwood factor $G_{\mathrm{L}}(k,t)$ is an even function on time, and we immediately recover the fluctuation formula (2) from (5). Furthermore, taking into account that $\mathscr{L}_{\mathrm{i}\omega}(-\dot{G}_{\mathrm{L}}(k,t)) = G_{\mathrm{L}}(k,0) - \mathrm{i}\omega\mathscr{L}_{\mathrm{i}\omega}(G_{\mathrm{L}}(k,t)) \equiv \mathscr{L}_{\mathrm{i}\omega}(C_{\mathrm{L}}(k,t))/\mathrm{i}\omega$ we obtain, in particular, that the static ($t = 0$) longitudinal Kirkwood factor $G_{\mathrm{L}}(k) \equiv G_{\mathrm{L}}(k,0)$ is connected with the dynamical Kirkwood factor of second order as

$$G_{\mathrm{L}}(k) = \lim_{\omega\to+0}\frac{\mathscr{L}_{\mathrm{i}\omega}(C_{\mathrm{L}}(k,t))}{\mathrm{i}\omega} = -\int_0^\infty tC_{\mathrm{L}}(k,t)\mathrm{d}t \ , \tag{8}$$

where the equality (8) holds for the infinite-system functions $g_{\mathrm{L}}(k)$ and $c_{\mathrm{L}}(k,t)$ as well.

Despite the difference, in general, between the longitudinal Kirkwood factors for the finite and infinite systems, we, nevertheless, can reproduce the infinite-system behaviour indirectly using the relations

$$\frac{1}{\mathscr{L}_{\mathrm{i}\omega}(\dot{g}_{\mathrm{L}}(k,t))} = \frac{1}{\mathscr{L}_{\mathrm{i}\omega}(\dot{G}_{\mathrm{L}}(k,t))} - hD(k)\ , \qquad \frac{\mathrm{i}\omega}{\mathscr{L}_{\mathrm{i}\omega}(c_{\mathrm{L}}(k,t))} = \frac{\mathrm{i}\omega}{\mathscr{L}_{\mathrm{i}\omega}(C_{\mathrm{L}}(k,t))} + hD(k)\ . \tag{9}$$

Taking into account the Laplace boundary theorem $\lim_{\omega\to\infty} \mathrm{i}\omega\mathscr{L}_{\mathrm{i}\omega}(\phi(t)) = \lim_{t\to 0}\phi(t)$, it can be shown from (9) that $\frac{\partial^2}{\partial t^2}G_{\mathrm{L}}(k,t)\Big|_{t=0} = \frac{\partial^2}{\partial t^2}g_{\mathrm{L}}(k,t)\Big|_{t=0}$ and $C_{\mathrm{L}}(k) = c_{\mathrm{L}}(k)$, respectively. So that, contrary to the usual Kirkwood factor $G_{\mathrm{L}}(k)$, the static Kirkwood factor of second order $C_{\mathrm{L}}(k)$ is free of boundary effects. The transverse function $c_{\mathrm{T}}(k,t)$ is equal to $C_{\mathrm{T}}(k,t)$ at arbitrary times, because $\boldsymbol{E}_{\mathrm{T}} = \boldsymbol{E}_0^{\mathrm{T}}$ for nonrelativistic systems, and it can be obtained in simulations directly without additional manipulations. Moreover, the static Kirkwood factors of second order $c_{\mathrm{L,T}}(k)$ are presented in analytical forms (see Appendix).

B. Transverse dielectric function and magnetic permittivity

We now consider an alternative approach to describe the electromagnetic properties of ISM systems. This approach is based on the separation of macroscopic currents into electric and magnetic parts in the limit $k, \omega \to 0$. Neglecting terms of order k^2, ω^2, $k\omega$ and higher, the averaged values for the operator of current density (3) can be evaluated in $(\boldsymbol{k},\omega)$-space as

$$\langle\hat{\boldsymbol{I}}(\boldsymbol{k},\omega)\rangle = \mathrm{i}c\boldsymbol{k}\times\langle\hat{\boldsymbol{\mathcal{M}}}(\omega)\rangle + \mathrm{i}\omega\langle\hat{\boldsymbol{\mathcal{P}}}(\omega)\rangle\ , \tag{10}$$

where $\hat{\boldsymbol{\mathcal{P}}}(\omega)$ and $\hat{\boldsymbol{\mathcal{M}}}(\omega)$ are frequency components of the total electric dipole moment $\hat{\boldsymbol{\mathcal{P}}}(t) = \sum_{i=1}^{N}\boldsymbol{d}_i(t)$ and the rotational part $\hat{\boldsymbol{\mathcal{M}}}(t) = \sum_{i=1}^{N}\boldsymbol{m}_i(t)$ of the magnetic dipole moment of the system, where $\boldsymbol{m}_i = \frac{1}{2c}\sum_{a=1}^{M} q_a\boldsymbol{\delta}_i^a\times\boldsymbol{v}_i^a$. In our notations $\boldsymbol{\delta}_i^a = \boldsymbol{r}_i^a - \boldsymbol{r}_i$ and $\boldsymbol{v}_i^a = \boldsymbol{V}_i^a - \boldsymbol{V}_i = \boldsymbol{\Omega}_i\times\boldsymbol{\delta}_i^a$ are the positions and velocities of sites relatively to the molecular centre of mass $\boldsymbol{r}_i$ and its velocity $\boldsymbol{V}_i$, respectively, and $\boldsymbol{\Omega}_i$ is the angular velocity of the ith molecule.

Despite the fact that the separation (10) is realized uniquely only in the macroscopic regime at small wavenumbers and frequencies [17], we shall apply it at the microscopic level of description and extend to arbitrary k and ω. Such an extension can be performed by writing (in $(\boldsymbol{k},t)$-representation)

$$\hat{\boldsymbol{I}}(\boldsymbol{k},t) = \mathrm{i}c\boldsymbol{k}\times\hat{\boldsymbol{\mathcal{M}}}(\boldsymbol{k},t) + \frac{\mathrm{d}}{\mathrm{d}t}\hat{\boldsymbol{\mathcal{P}}}(\boldsymbol{k},t)\ , \tag{11}$$

where $\hat{\boldsymbol{\mathcal{P}}}(\boldsymbol{k},t)$ and $\hat{\boldsymbol{\mathcal{M}}}(\boldsymbol{k},t)$ are appropriate dynamical variables associated with the microscopic polarization and magnetization densities, respectively. In view of equations (3), (10) and (11), these variables should satisfy the limiting transitions $\lim_{k\to 0}\hat{\boldsymbol{\mathcal{P}}}(\boldsymbol{k},t) = \hat{\boldsymbol{\mathcal{P}}}(t)$ and $\lim_{k\to 0}\hat{\boldsymbol{\mathcal{M}}}(\boldsymbol{k},t) = \hat{\boldsymbol{\mathcal{M}}}(t)$. Moreover, taking the scalar product of equations (3) and (11) on unit vector $\hat{\boldsymbol{k}}$ yields the condition $\hat{\boldsymbol{\mathcal{P}}}_{\mathrm{L}}(\boldsymbol{k},t) = \hat{\boldsymbol{P}}_{\mathrm{L}}(\boldsymbol{k},t)$, where the equality $\hat{\boldsymbol{k}}\cdot[\boldsymbol{k}\times\hat{\boldsymbol{\mathcal{M}}}] = 0$ has been used.

The explicit expression for $\hat{\boldsymbol{\mathcal{P}}}(\boldsymbol{k},t)$ can be derived using the following procedure [16]. Let us split the operator $\hat{Q}(\boldsymbol{k},t) = \sum_{i=1}^{N}\hat{q}_i(\boldsymbol{k},t)\mathrm{e}^{-\mathrm{i}\boldsymbol{k}\cdot\boldsymbol{r}_i(t)}$ of charge density into its molecular components $\hat{q}_i(\boldsymbol{k},t) = \sum_{a=1}^{M} q_a\mathrm{e}^{-\mathrm{i}\boldsymbol{k}\cdot\boldsymbol{\delta}_i^a(t)}$. Then it is natural to introduce the total microscopic polarization density as $\hat{\boldsymbol{\mathcal{P}}}(\boldsymbol{k},t) = \sum_{i=1}^{N}\hat{\boldsymbol{p}}_i(\boldsymbol{k},t)\mathrm{e}^{-\mathrm{i}\boldsymbol{k}\cdot\boldsymbol{r}_i(t)}$, where $\hat{\boldsymbol{p}}_i(\boldsymbol{k},t)$ is the polarization density of the ith molecule, and to extend the relation $\hat{Q}(\boldsymbol{k},t) = -\mathrm{i}\boldsymbol{k}\cdot\hat{\boldsymbol{P}}(\boldsymbol{k},t)$ to the molecular level, i.e., $\hat{q}_i(\boldsymbol{k},t) = -\mathrm{i}\boldsymbol{k}\cdot\hat{\boldsymbol{p}}_i(\boldsymbol{k},t)$. Further, taking into account the identity $\mathrm{e}^{\xi} = 1 + \xi\int_0^1 \mathrm{d}u\mathrm{e}^{u\xi}$, applied to the quantity $\xi = -\mathrm{i}\boldsymbol{k}\cdot\boldsymbol{\delta}_i^a$, and using the molecular charge electroneutrality $\sum_{a=1}^{M} q_a = 0$, we present $q_i(\boldsymbol{k},t)$ as $-\mathrm{i}\boldsymbol{k}\cdot\sum_{a=1}^{M} q_a\boldsymbol{\delta}_i^a(t)\int_0^1 \mathrm{d}u\mathrm{e}^{-\mathrm{i}u\boldsymbol{k}\cdot\boldsymbol{\delta}_i^a(t)}$. The last expression leads to $\hat{\boldsymbol{p}}_i(\boldsymbol{k},t) = \sum_{a=1}^{M} q_a\boldsymbol{\delta}_i^a(t)\int_0^1 \mathrm{d}u\mathrm{e}^{-\mathrm{i}u\boldsymbol{k}\cdot\boldsymbol{\delta}_i^a(t)}$ and, therefore,

$$\hat{\boldsymbol{\mathcal{P}}}(\boldsymbol{k},t) = \sum_{i=1}^{N}\sum_{a=1}^{M} q_a\boldsymbol{\delta}_i^a(t)\frac{\mathrm{e}^{-\mathrm{i}\boldsymbol{k}\cdot\boldsymbol{\delta}_i^a(t)} - 1}{-\mathrm{i}\boldsymbol{k}\cdot\boldsymbol{\delta}_i^a(t)}\,\mathrm{e}^{-\mathrm{i}\boldsymbol{k}\cdot\boldsymbol{r}_i(t)}\ . \tag{12}$$

Of course, such a procedure does not define $\hat{\boldsymbol{\mathcal{P}}}(\boldsymbol{k},t)$ uniquely, because q_i is indifferent to the transverse part of $\hat{\boldsymbol{p}}_i$. Nevertheless, it was assumed [16] to adopt equation (12) as the definition of microscopic polarization density for ISM fluids. From this definition it immediately follows that the longitudinal components of vectors $\hat{\boldsymbol{P}}$ and $\hat{\boldsymbol{\mathcal{P}}}$ coincide completely between themselves at arbitrary wavevectors.

Since the functions $\hat{\boldsymbol{I}}(\boldsymbol{k},t)$ and $\hat{\boldsymbol{\mathcal{P}}}(\boldsymbol{k},t)$ are already defined, equation (11) allows one to determine the transverse part of microscopic magnetization density,

$$\hat{\boldsymbol{\mathcal{M}}}_{\mathrm{T}}(\boldsymbol{k},t) = \hat{\boldsymbol{k}}\times[\hat{\boldsymbol{\mathcal{M}}}(\boldsymbol{k},t)\times\hat{\boldsymbol{k}}] = \frac{1}{\mathrm{i}ck}\Big(\hat{\boldsymbol{I}}(\boldsymbol{k},t) - \frac{\mathrm{d}}{\mathrm{d}t}\hat{\boldsymbol{\mathcal{P}}}(\boldsymbol{k},t)\Big)\times\hat{\boldsymbol{k}}\ . \tag{13}$$

It can be verified using equations (3), (12) and (13) that in the infinite-wavelength limit $k\to 0$ the functions $\hat{\boldsymbol{\mathcal{P}}}(\boldsymbol{k},t)$ and $\hat{\boldsymbol{\mathcal{M}}}_{\mathrm{T}}(\boldsymbol{k},t)$ tend to the true microscopic variables $\sum_{i=1}^{N}\boldsymbol{d}_i(t) = \sum_{i=1}^{N}\sum_{a=1}^{M} q_a\boldsymbol{\delta}_i^a(t)$ and $\hat{\boldsymbol{k}}\times\sum_{i=1}^{N}[\boldsymbol{m}_i(t)\times\hat{\boldsymbol{k}}]$ which correspond to the electric and rotational magnetic dipole moments of the system, respectively. However, at $k\neq 0$ the vectors $\hat{\boldsymbol{\mathcal{P}}}(\boldsymbol{k},t)$ (as well as $\hat{\boldsymbol{P}}(\boldsymbol{k},t)$) and $\hat{\boldsymbol{\mathcal{M}}}_{\mathrm{T}}(\boldsymbol{k},t)$ take into account explicitly the charge distribution within a finite spatial extend of the molecule and, therefore, they can

not longer be associated with the point dipole densities $\hat{\mathscr{P}}(\boldsymbol{k},t)=\sum_{i=1}^{N}\boldsymbol{d}_i(t)\mathrm{e}^{-\mathrm{i}\boldsymbol{k}\cdot\boldsymbol{r}_i(t)}$ and $\hat{\mathscr{M}}_{\mathrm{T}}(\boldsymbol{k},t)=\hat{\boldsymbol{k}}\times\sum_{i=1}^{N}[\boldsymbol{m}_i(t)\times\hat{\boldsymbol{k}}]\mathrm{e}^{-\mathrm{i}\boldsymbol{k}\cdot\boldsymbol{r}_i(t)}$. For purely dipole models, when $|q_a|\to\infty$ and $\max_a|\boldsymbol{\delta}_i^a|\to 0$, provided $d\to\mathrm{const}$, we obtain $\hat{\boldsymbol{\mathcal{P}}}(\boldsymbol{k},t)\to\hat{\mathscr{P}}(\boldsymbol{k},t)$, but $\hat{\mathscr{M}}(\boldsymbol{k},t)\to 0$ because of $\boldsymbol{m}_i\to 0$ and, thus, there is no magnetic response in this case, i.e., $\hat{\boldsymbol{\mathcal{P}}}(\boldsymbol{k},t)\equiv\hat{\boldsymbol{P}}(\boldsymbol{k},t)$ at arbitrary wavevectors.

In the present approach the electric phenomena are described by the frequency-dependent dielectric functions $\epsilon_{\mathrm{L,T}}(k,\omega)$, while the magnetic state is determined by the magnetic permittivity $\mu(k,\omega)\equiv\mu_{\mathrm{T}}(k,\omega)$ (for the system under consideration the longitudinal magnetic susceptibility is absent). These quantities are defined via the material relations $\boldsymbol{\mathcal{P}}_{\mathrm{L,T}}(\boldsymbol{k},\omega)=\frac{1}{4\pi}(\epsilon_{\mathrm{L,T}}(k,\omega)-1)\boldsymbol{E}_{\mathrm{L,T}}(\boldsymbol{k},\omega)$ and $\boldsymbol{\mathcal{M}}_{\mathrm{T}}(\boldsymbol{k},\omega)=\frac{1}{4\pi}(\mu(k,\omega)-1)\boldsymbol{H}_{\mathrm{T}}(\boldsymbol{k},\omega)$, where the statistical averaging of $\boldsymbol{\mathcal{P}}=\langle\hat{\boldsymbol{\mathcal{P}}}\rangle$ and $\boldsymbol{\mathcal{M}}=\langle\hat{\boldsymbol{\mathcal{M}}}\rangle$ is performed in the presence of external electric $\boldsymbol{E}_0$ and magnetic $\boldsymbol{H}_0$ fields. We mention that for nonrelativistic systems the total magnetic field $\boldsymbol{H}$ is indistinguishable from the external field, i.e., $\boldsymbol{H}_{\mathrm{T}}=\boldsymbol{H}_0^{\mathrm{T}}$. We stress also that it is necessary to distinguish the generalized dielectric tensor $\varepsilon_{\mathrm{L,T}}(k,\omega)$ corresponding to the total current $\boldsymbol{I}=\mathrm{d}\boldsymbol{P}/\mathrm{d}t$ from the dielectric functions $\epsilon_{\mathrm{L,T}}(k,\omega)$ related to the electric part $\mathrm{d}\boldsymbol{\mathcal{P}}/\mathrm{d}t$ of $\boldsymbol{I}$. It is obvious that $\epsilon_{\mathrm{L}}(k,\omega)\equiv\varepsilon_{\mathrm{L}}(k,\omega)$ because of $\hat{\boldsymbol{\mathcal{P}}}_{\mathrm{L}}(\boldsymbol{k},t)=\hat{\boldsymbol{P}}_{\mathrm{L}}(\boldsymbol{k},t)$, but $\epsilon_{\mathrm{T}}(k,\omega)\neq\varepsilon_{\mathrm{T}}(k,\omega)$ since, in general, $\hat{\boldsymbol{\mathcal{P}}}_{\mathrm{T}}(\boldsymbol{k},t)\neq\hat{\boldsymbol{P}}_{\mathrm{T}}(\boldsymbol{k},t)$. The fluctuation formula for the transverse dielectric function $\epsilon_{\mathrm{T}}(k,\omega)$ can be obtained in a similar way as for permittivities $\varepsilon_{\mathrm{L,T}}(k,\omega)$ (see the preceding subsection and Ref. [1]). The result is

$$\epsilon_{\mathrm{T}}(k,\omega)-1=h\mathscr{L}_{\mathrm{i}\omega}(-\dot{g}_{\mathrm{T}}(k,t))\ , \tag{14}$$

where the infinite-system correlation function $g_{\mathrm{T}}(k,t)=\left\langle\hat{\boldsymbol{\mathcal{P}}}_{\mathrm{T}}(\boldsymbol{k},0)\cdot\hat{\boldsymbol{\mathcal{P}}}_{\mathrm{T}}(-\boldsymbol{k},t)\right\rangle_0\Big/2Nd^2$ can be evaluated in simulation directly, because of $\boldsymbol{E}_{\mathrm{T}}=\boldsymbol{E}_0^{\mathrm{T}}$.

Finally, we would like to discuss about a relationship of the two approaches presented in more detail. In the abbreviated approach the electric and magnetic parts in the total current are not distinguished from one another. In such a situation the magnetic part is included into the generalized $\hat{\boldsymbol{P}}$-vector (3) and the transverse electromagnetic fluctuations are described by one function only, namely, by the generalized dielectric constant $\varepsilon_{\mathrm{T}}(k,\omega)$. This including indeed can be realized because at $k,\omega\neq 0$ magnetic fields are expressed in terms of electric fields $\boldsymbol{E}$ using the Maxwell equation $c\,\mathrm{rot}\boldsymbol{E}=-\partial\boldsymbol{B}/\partial t$ in $(\boldsymbol{k},\omega)$-representation, i.e., $c\boldsymbol{k}\times\boldsymbol{E}(\boldsymbol{k},\omega)=-\omega\boldsymbol{B}_{\mathrm{T}}(\boldsymbol{k},\omega)$, where $\boldsymbol{B}_{\mathrm{T}}(\boldsymbol{k},\omega)=\mu(k,\omega)\boldsymbol{H}_{\mathrm{T}}(\boldsymbol{k},\omega)$. At the same time, the extended approach involves two quantities, $\epsilon_{\mathrm{T}}(k,\omega)$ and $\mu(k,\omega)$, for the description. As far as these two approaches deal with the same microscopic current,

the quantities $\varepsilon_{\mathrm{T}}(k,\omega)$, $\epsilon_{\mathrm{T}}(k,\omega)$ and $\mu(k,\omega)$ are not independent. The corresponding relation can be found comparing the right-hand sides of equations (3) and (11) between themselves and using material equations. Then one obtains

$$\varepsilon_{\mathrm{T}}(k,\omega) = \epsilon_{\mathrm{T}}(k,\omega) + \frac{c^2k^2}{\omega^2}\frac{\mu(k,\omega)-1}{\mu(k,\omega)} \tag{15}$$

and, therefore, the wavevector- and frequency-dependent magnetic permittivity is caused by the difference between functions $\varepsilon_{\mathrm{T}}(k,\omega)$ and $\epsilon_{\mathrm{T}}(k,\omega)$.

The simplest way to obtain the explicit fluctuation formula for the magnetic permittivity is based on relation (15) and fluctuation formulas (6) and (14) for $\varepsilon_{\mathrm{T}}(k,\omega)$ and $\epsilon_{\mathrm{T}}(k,\omega)$. In view of equation (11), the transverse current autocorrelation function $c_{\mathrm{T}}(k,t)$ (7), appearing in fluctuation formula (6) for $\varepsilon_{\mathrm{T}}(k,\omega)$, can be expressed in terms of the polarization $g_{\mathrm{T}}(k,t)$ and magnetization $s_{\mathrm{T}}(k,t) = \left\langle \hat{\boldsymbol{\mathcal{M}}}_{\mathrm{T}}(\boldsymbol{k},0)\cdot\hat{\boldsymbol{\mathcal{M}}}_{\mathrm{T}}(-\boldsymbol{k},t)\right\rangle_0 \big/ 2Nd^2$ correlation functions as $c_{\mathrm{T}}(k,t) = c^2k^2 s_{\mathrm{T}}(k,t) - \partial^2 g_{\mathrm{T}}(k,t)/\partial t^2$. It is necessary to point out that for spatially homogeneous systems, as in our case, the cross function $\left\langle \hat{\boldsymbol{\mathcal{P}}}_{\mathrm{T}}\cdot\hat{\boldsymbol{\mathcal{M}}}_{\mathrm{T}}\right\rangle_0$, corresponding to correlations between the polarization and magnetization vectors, does not appear and it is equal to zero for arbitrary wavenumbers and times. Indeed, let us direct $\hat{\boldsymbol{k}}$-vector along z-axis of the laboratory reference frame. Then it follows from the structure of equation (11) that $\hat{\boldsymbol{\mathcal{P}}}_{\mathrm{T}}\cdot\hat{\boldsymbol{\mathcal{M}}}_{\mathrm{T}} = \frac{1}{2}(\hat{\mathcal{P}}_x\hat{\mathcal{M}}_y + \hat{\mathcal{P}}_y\hat{\mathcal{M}}_x)$, where $\hat{\mathcal{P}}_{x,y}$ and $\hat{\mathcal{M}}_{x,y}$ are the xth and yth components of vectors $\hat{\boldsymbol{\mathcal{P}}}$ and $\hat{\boldsymbol{\mathcal{M}}}$, respectively. Since the fluctuations of vector quantities in different directions of the fixed laboratory frame are statistically independent at equilibrium, we have that $\left\langle \hat{\boldsymbol{\mathcal{P}}}_{\mathrm{T}}(\boldsymbol{k},0)\cdot\hat{\boldsymbol{\mathcal{M}}}_{\mathrm{T}}(-\boldsymbol{k},t)\right\rangle_0 = 0$. Further, as far as the relativistic effects have been neglected, the functions $\varepsilon_{\mathrm{T}}(k,\omega)$ and $\epsilon_{\mathrm{T}}(k,\omega)$ are evaluated via fluctuation formulas (6) and (14), in fact, with a precision of order $(v/c)^2$, where $v \ll c$ is the mean heat velocity of atoms. This leads to uncertainties of order c^{-4} in the evaluation of $\mu(k,\omega)$ via relation (15). Within the same precision we can putt $(\mu(k,\omega)-1)/\mu(k,\omega) \approx \mu(k,\omega)-1$, so that the desired fluctuation formula is

$$\mu(k,\omega) - 1 = -\mathrm{i}\omega h\mathscr{L}_{\mathrm{i}\omega}(s_{\mathrm{T}}(k,t)) + \mathcal{O}(c^{-4}) \ , \tag{16}$$

where the infinite-system function $s_{\mathrm{T}}(k,t)$ can be reproduced directly in simulation, because of $\boldsymbol{H}_{\mathrm{T}} = \boldsymbol{H}_0^{\mathrm{T}}$.

From the afore said, it is obvious that the two approaches are completely equivalent for the evaluations of the generalized dielectric permittivity $\varepsilon_{\mathrm{T}}(k,\omega)$ and they can be applied with equal successes to theoretical applications. However, the extended description is only the way to determine the magnetic permittivity at $k \neq 0$. It is interesting to

point out also that in the infinite-wavelength regime $k \to 0$, the functions $\varepsilon_{\rm L}(k,\omega) \equiv \epsilon_{\rm L}(k,\omega)$ and $\epsilon_{\rm T}(k,\omega)$ differ between themselves by terms of order k^4 and higher, i.e., $\lim_{k\to 0}[\varepsilon_{\rm L}(k,\omega) - \epsilon_{\rm T}(k,\omega)]/k^2 = 0$. This statement can be examined on the basis of fluctuation formulas (2), (14) and explicit expression (12) for microscopic variable $\hat{\boldsymbol{\mathcal{P}}}$. Then, using relation (15), we obtain that in the abbreviated description the frequency-dependent magnetic permittivity $\mu(\omega) = \lim_{k\to 0}\mu(k,\omega)$ appears as a result of the limiting transition

$$1 - \frac{1}{\mu(\omega)} = \frac{\omega^2}{c^2}\lim_{k\to 0}\frac{\varepsilon_{\rm T}(k,\omega) - \varepsilon_{\rm L}(k,\omega)}{k^2} \tag{17}$$

which shows that differences between the longitudinal and transverse components of the generalized dielectric tensor $\boldsymbol{\varepsilon}(\boldsymbol{k},\omega)$ in the infinite-wavelength limit are caused by magnetic properties of the system [17]. Thus, in the presence of spatially inhomogeneous fields, the electromagnetic state is determined by the generalized transverse $\varepsilon_{\rm T}(k,\omega)$ and longitudinal $\varepsilon_{\rm L}(k,\omega)$ dielectric functions. When the spatial dispersion can be neglected, all electric and magnetic phenomena in the system are uniquely described by two quantities again, namely, by the frequency-dependent dielectric constant $\varepsilon(\omega) = \lim_{k\to 0}\varepsilon_{\rm L}(k,\omega) = \lim_{k\to 0}\epsilon_{\rm L,T}(k,\omega)$ and magnetic permittivity $\mu(\omega)$.

III. NUMERICAL CALCULATIONS FOR THE TIP4P MODEL

Molecular dynamics simulations were carried out for the TIP4P potential [21] at a density of 1 g/cm^3 and at a temperature of $T = 293$ K. We performed two runs corresponding to the ISRF [3] and Ewald [22] geometries. The equations of motion were integrated on the basis of a matrix method [23] with a time step of 2 fs. The observation times over the equilibrium state were 500 000 and 1 000 000 time steps for the Ewald and ISRF geometry, respectively. The time correlation functions were calculated in an interval of 2 ps for the wavenumbers $k = [0, 1, \ldots, 300]k_{\rm min}$, where $k_{\rm min} = 2\pi/L = 0.319\text{Å}^{-1}$ and L is the length of the simulation box edge. The parameters $\eta = 5.76/L$ and $k_{\rm max} = 5k_{\rm min}$ have been used in the Ewald summation of the Coulomb forces. Other details of the simulations are similar to those reported earlier [1].

A. Dielectric properties

The longitudinal component $G_{\rm L}(k)$ of the static wavevector-dependent Kirkwood factor, calculated in the simulations within the Ewald and ISRF geometries, is shown

in fig. 1a by the full squares and dashed curve, respectively. Since, in the ISRF geometry the function $D(k) = 3j_1(kR)/(kR)$ differs from zero considerably, especially at small wavenumbers, to evaluate the infinite-system Kirkwood factor $g_{\rm L}(k)$ the performance of self-consistent transformations (9) is necessary. This result is plotted by the solid curve. Within the Ewald geometry [22] the function $D(k)$ is equal to $1 - \int_0^R kj_1(k\rho)\Big(\mathrm{erfc}(\eta\rho) + \frac{2\eta}{\sqrt{\pi}}\rho\exp(-\eta^2\rho^2)\Big)\mathrm{d}\rho - \exp(-k^2/4\eta^2)$, where the last term is to be included only if $0 < k \leq k_{\max}$, and at the given parameters of the summation $D(k)$ is very close to zero ($\max_{k\neq 0}|D(k)| < 0.00005$). So that the infinite-system Kirkwood factor is equivalent to that, obtained in the simulations (excepting the case $k = 0$). As we can see from the figure, the both Ewald and ISRF methods lead to identical results for $g_{\rm L}(k)$. The static Kirkwood factor of second order, $C_{\rm L,T}(k)$ (equation (7)), is presented in fig. 1b. As was pointed out earlier, this function is free of boundary conditions and the infinite-system dependence $c_{\rm L,T}(k)$ can be reproduced directly in the simulations. This is confirmed by our calculations performed in the different geometries. The obtained values for $C_{\rm L,T}(k)$ are practically indistinguishable from those evaluated from analytical expressions (A5) for $c_{\rm L,T}(k)$. They differ from one another within statistical noise only.

Samples of the normalized, dynamical Kirkwood factor of second order, $\Psi_{\rm L,T}(k,t) = C_{\rm L,T}(k,t)/C_{\rm L,T}(k)$, are plotted in fig. 2. The longitudinal infinite-system functions $c_{\rm L}(k,t)/c_{\rm L}(k)$ within the ISRF geometry at arbitrary wavenumbers and for the Ewald geometry at $k = 0$ have been determined applying the inverse Laplace transform to relations (9), whereas $c_{\rm T}(k,t) = C_{\rm T}(k,t)$ for the transverse functions. We note that $C_{\rm L}(k,t) = C_{\rm T}(k,t)$ at $k = 0$. At $k \neq 0$ the Ewald method reproduces directly the infinite-system behaviour. The agreement between the two sets of data for $c_{\rm L,T}(k,t)$, corresponding to the ISRF and Ewald geometries, is quite good. It is worth to remark also that the zeroth time moment $\int_0^\infty c_{\rm L}(k,t)\mathrm{d}t$ is equal to zero for arbitrary wavenumbers (this statement directly follows from equality (8)), whereas, in general, $\int_0^\infty c_{\rm T}(k,t)\mathrm{d}t \neq 0$ in the case of transverse total current fluctuations.

As was shown in the preceding section, the longitudinal static Kirkwood factor $G_{\rm L}(k)$ of order zero can be determined through the first time moment on the dynamical Kirkwood factor $C_{\rm L}(k,t)$ of second order (see equation (8)). The calculated in such a way function $G_{\rm L}(k)$ within the ISRF geometry and the function $g_{\rm L}(k)$ (via $c_{\rm L}(k,t)$) using the Ewald method are presented in fig. 1a by rotated and direct crosses, respectively. As we see from the calculations, these functions differ considerably from those obtained in the usual way. This difference occurs because the calculation of the expression $\mathscr{L}_{\mathrm{i}\omega}(C_{\rm L}(k,t))/\mathrm{i}\omega$ at small

frequencies is very sensitive to the precision of the evaluation of $\mathscr{L}_{\mathrm{i}\omega}(C_{\mathrm{L}}(k,t))$ (dividing two small quantities between themselves). The problem is complicated additionally because this evaluation requires a numerical integration of time correlation functions which are defined in simulations approximately within a statistical noise. Therefore, this method is not recommended for the investigation of the longitudinal dielectric constant at low frequency values. However, in the opposite infinite-frequency limit, the calculation via equation (5) can be more convenient than using the usual way (2). For example, in this limit, where $\varepsilon_{\mathrm{L}}(k,\omega) \to 1$, we obtain from (2) that $\mathscr{L}_{\mathrm{i}\omega}(-\dot{g}_{\mathrm{L}}(k,t)) = g_{\mathrm{L}}(k) - \mathrm{i}\omega\mathscr{L}_{\mathrm{i}\omega}(g_{\mathrm{L}}(k,t)) \to 0$. The exact computation of $\mathrm{i}\omega\mathscr{L}_{\mathrm{i}\omega}(g_{\mathrm{L}}(k,t))$ at large frequencies may lead to a problem (multiplying of quantities with significantly different orders). This situation is absent in the case when fluctuation formula (5) is applied to calculations.

And now we are in a position to discuss a behaviour of the generalized dielectric permittivity in the low frequency regime $\omega \to 0$. As was established previously [1], the real part of the longitudinal dielectric permittivity $\varepsilon_{\mathrm{L}}(k,\omega)$ at $\omega \to 0$ tends to its static value $\varepsilon_{\mathrm{L}}(k)$, while the imaginary part vanishes at arbitrary wavenumbers except the cases of two singularities, where $\varepsilon_{\mathrm{L}}(k) = \pm\infty$. In the singularity range, the real part of the dielectric permittivity is equal to zero, whereas the imaginary part behaves as $-\mathrm{i}/\omega\tau_{\mathrm{L}}^{\mathrm{cor}}(k)$, where $\tau_{\mathrm{L}}^{\mathrm{cor}}(k) = \int_0^\infty \mathrm{d}t\, g_{\mathrm{L}}(k,t)/g_{\mathrm{L}}(k)$ is the longitudinal correlation time. Such a behaviour of the longitudinal dielectric constant causes the coefficient $\sigma_{\mathrm{L}}(k) = \lim_{\omega\to 0}\sigma_{\mathrm{L}}(k,\omega) = 1/4\pi\tau_{\mathrm{L}}^{\mathrm{cor}}(k) \neq 0$ for longitudinal conductivity in the singularity regions, whereas outside the singularities $\sigma_{\mathrm{L}}(k) = 0$. The existence of a nonvanishing coefficient in the static limit does not lead, however, to macroscopic currents (as it must be for dielectrics), because the total longitudinal field in the system vanishes when $|\varepsilon_{\mathrm{L}}(k)| \to \infty$.

In the case of transverse fluctuations the pattern is qualitatively different. According to fluctuation formula (6), the transverse dielectric permittivity $\varepsilon_{\mathrm{T}}(k,\omega)$ at low frequencies behaves as $1 + \lim_{\omega\to 0} h\mathscr{L}_{\mathrm{i}\omega}(c_{\mathrm{T}}(k,t))/\mathrm{i}\omega = \varepsilon'(k) - \mathrm{i}\varepsilon''(k)$, where $\varepsilon'(k) = \Re\lim_{\omega\to 0}\varepsilon_{\mathrm{T}}(k,\omega) = 1 - h\int_0^\infty tc_{\mathrm{T}}(k,t)\mathrm{d}t$ denotes the real part, whereas the imaginary part $\varepsilon''(k) = -\Im\lim_{\omega\to 0}\varepsilon_{\mathrm{T}}(k,\omega) = 4\pi\sigma_{\mathrm{T}}(k)/\omega$ is described by the wavevector-dependent generalized transverse conductivity $\sigma_{\mathrm{T}}(k) = \frac{h}{4\pi}\lim_{\omega\to 0}\mathscr{L}_{\mathrm{i}\omega}(c_{\mathrm{T}}(k,t)) = \frac{h}{4\pi}\int_0^\infty c_{\mathrm{T}}(k,t)\mathrm{d}t$. We mention that the precision of calculations of the generalized dielectric permittivity at low frequencies is very sensitive to statistical uncertainties of data for total current fluctuations $c_{\mathrm{L,T}}(k,t)$ obtained in computer experiment. An additional source of errors is the truncation of long time tails in correlation functions at numerical integration. As a consequence, we could not provide a satisfactory reproduction of $\varepsilon_{\mathrm{T}}(k,\omega)$ directly in terms

of $c_{\rm T}(k,t)$, especially at small wavevectors and in the case of the Ewald method, where the length of the simulation was twice smaller than for the ISRF geometry. For the last reason, all other results will be presented in the ISRF geometry only. The computations show that a much more reliable evaluation can be performed when the generalized permittivity $\varepsilon_{\rm T}(k,\omega)$ is found via relation (15), i.e., in terms of the transverse dielectric $\epsilon_{\rm T}(k,\omega)$ and magnetic $\mu(k,\omega)$ functions which correspond to polarization $g_{\rm T}(k,t)$ and magnetization $s_{\rm T}(k,t)$ fluctuations. Then in view of (16), relation (15) transforms at $\omega \to 0$ to

$$\lim_{\omega\to 0} \varepsilon_{\rm T}(k,\omega) = \epsilon_{\rm T}(k) - {\rm i}h\frac{c^2k^2}{\omega} \lim_{\omega\to 0} \mathscr{L}_{{\rm i}\omega}(s_{\rm T}(k,t)) + \mathcal{O}(\omega, c^{-4}) \ , \tag{18}$$

where $\epsilon_{\rm T}(k) = \lim_{\omega\to 0} \epsilon_{\rm T}(k,\omega) = 1 + hg_{\rm T}(k)$ is the static dielectric function and $g_{\rm T}(k) = \lim_{t\to 0} g_{\rm T}(k,t)$. From equality (18) we immediately obtain that $\varepsilon'_{\rm T}(k) = \epsilon_{\rm T}(k) - hc^2k^2 \int_0^\infty ts_{\rm T}(k,t){\rm d}t$ and $\varepsilon''_{\rm T}(k) = 4\pi\sigma_{\rm T}(k)/\omega$ with $\sigma_{\rm T}(k) = \frac{h}{4\pi}c^2k^2 \int_0^\infty s_{\rm T}(k,t){\rm d}t$.

The wavevector-dependent dielectric function $\epsilon_{\rm T}(k)$ is shown in fig. 3a by the solid curve. In the infinite-wavelength limit $k \to 0$, this function tends to the value $\varepsilon_0 = \lim_{k\to 0} \varepsilon_{\rm L}(k) \approx 53$, corresponding to the usual dielectric constant in the absence of any spatial and time dispersions. It is equal to unity in the opposite limit $k \to \infty$, indicating that the system exhibits no dielectric response with respect to strong spatially inhomogeneous electric fields. The dielectric function $\epsilon_{\rm T}^{\rm PD}(k) = 1 + hg_{\rm T}^{\rm PD}(k)$, calculated in the point dipole (PD) approximation $g_{\rm T}^{\rm PD}(k) = \langle \hat{\mathscr{P}}_{\rm T}(\boldsymbol{k},0)\cdot\hat{\mathscr{P}}_{\rm T}(-\boldsymbol{k},0)\rangle_0 \big/ 2Nd^2$, is presented in fig. 3a by the dashed curve. As can be seen from the figure, this function behaves like that for a Stockmayer fluid [13]. The PD approach is suitable for the reproduction of $\epsilon_{\rm T}(k)$ at very small wavenumbers only, namely, at $k \ll \pi/r \sim 3.4{\rm \AA}^{-1}$, where $r = \max_a |\boldsymbol{\delta}_i^a| \sim 0.92{\rm \AA}$ denotes the radius of the TIP4P molecule. In this wavevector range $\hat{\boldsymbol{\mathcal{P}}} \approx \hat{\mathscr{P}}$ and the spatial extend of charges within the molecule can be not taken into account when constructing the operator of microscopic polarization density. At greater wavevectors, the PD function differs drastically from that obtained within the exact interaction site description. In particular, the dielectric function $\epsilon_{\rm T}^{\rm PD}(k)$ tends to the wrong Onsager value $1 + h/3 = 17.4$ in the infinite-wavevector limit $k \to \infty$.

The wavevector-dependent coefficient $\sigma_{\rm T}(k)$ of transverse conductivity has been computed in two ways, namely, using the relations $\frac{h}{4\pi} \int_0^\infty c_{\rm T}(k,t){\rm d}t$ and $\frac{h}{4\pi}c^2k^2 \int_0^\infty s_{\rm T}(k,t){\rm d}t$. The corresponding results are shown in fig. 3b by open circles and the solid curve, respectively. These two approaches are mathematically equivalent, but may lead to different results in numerical calculations. For instance, the exact infinite-wavelength behaviour $\gamma k^2/4\pi$ of function $\sigma_{\rm T}(k)$, where $\gamma = hc^2 \lim_{k\to 0} \int_0^\infty s_{\rm T}(k,t){\rm d}t$, has been reproduced ex-

actly by us only in the second approach which, therefore, should be considered as a more preferable method of the calculations. As we can see from the figure, the coefficient of transverse conductivity $\sigma_{\rm T}(k)$ takes nonzero values for arbitrary nonzero wavevectors, contrary to the longitudinal conductivity.

It is necessary to stress that the transverse dielectric permittivity $\varepsilon_{\rm T}(k,\omega)$ has a singularity when both wavevector and frequency go to zero. The asymptotic behaviour near the singularity can be obtained on the basis of equation (18) using the equality $\lim_{k\to 0}\varepsilon'_{\rm T}(k) = \lim_{k\to 0}\epsilon_{\rm T}(k) = \varepsilon_0$. Then one finds that $\lim_{k,\omega\to 0}\varepsilon_{\rm T}(k,\omega) = \varepsilon_0 - {\rm i}\gamma k^2/\omega$. From the last expansion it is easy to see that $\varepsilon_{\rm T}(k,\omega)$ is a discontinuous function and its value depends on the order of the limiting transitions $k,\omega\to 0$, i.e., $\lim_{\omega\to 0}\lim_{k\to 0}\varepsilon_{\rm T}(k,\omega) = \varepsilon_0$ but $\lim_{k\to 0}\lim_{\omega\to 0}\varepsilon_{\rm T}(k,\omega) = -{\rm i}\infty$. As in the case of longitudinal fluctuations, the singularity of $\varepsilon_{\rm T}(k,\omega)$ does not lead to singularities in observing quantities and does not break the physical requirements imposed on dielectrics. In particular, the macroscopic current $\boldsymbol{I}_{\rm T}(\boldsymbol{k},\omega)$ does not appear at $\omega\to 0$, despite the fact that the coefficient $\sigma_{\rm T}(k,\omega)$ of the polarization conductivity accepts nonzero values at $k\neq 0$. Indeed, by the definition $\boldsymbol{I}_{\rm T}(\boldsymbol{k},\omega) = \sigma_{\rm T}(k,\omega)\boldsymbol{E}_{\rm T}(\boldsymbol{k},\omega)$, where the transverse electric field can be defined according to the Maxwell equation via the magnetic field as $\boldsymbol{E}_{\rm T}(\boldsymbol{k},\omega) = -\frac{\omega}{ck}\boldsymbol{B}(\boldsymbol{k},\omega)\times\hat{\boldsymbol{k}}$, so that the current vanishes as $\sim\omega$ at $\omega\to 0$. If k tends to zero additionally, we obtain, taking into account the asymptotic values $\gamma k^2\big/4\pi$ of $\sigma_{\rm T}(k,\omega)$, that $\lim_{k,\omega\to 0}\boldsymbol{I}_{\rm T}(\boldsymbol{k},\omega) = -\gamma k\omega\boldsymbol{B}(\boldsymbol{k})\times\hat{\boldsymbol{k}}\big/4\pi c\to 0$, where $\boldsymbol{B}(\boldsymbol{k}) = \lim_{\omega\to 0}\boldsymbol{B}(\boldsymbol{k},\omega)$, and the macroscopic current goes to zero again without any singularities.

At small frequencies, the partial contributions of the transverse component of dielectric functions into observing quantities are small (proportional to ω) with respect to the corresponding contributions of the longitudinal part. That is why the functions $\epsilon_{\rm T}(k)$ and $\sigma_{\rm T}(k)$, describing the wavevector dependence of $\epsilon_{\rm T}(k,\omega)$ and $\varepsilon_{\rm T}(k,\omega)$ in this frequency range, have not so important physical meaning as the static longitudinal dielectric permittivity $\varepsilon_{\rm L}(k)$. Moreover, since static electric fields are purely longitudinal, the response associated with $\epsilon_{\rm T}(k)$ and $\sigma_{\rm T}(k)$ cannot be realized phenomenologically in a homogeneous isotropic medium, except as the limits

$$\epsilon_{\rm T}(k) = \lim_{\omega\to 0}\left[1 + 4\pi\frac{\mathcal{P}_{\rm T}(k,\omega)}{E_{\rm T}(k,\omega)}\right] , \qquad \sigma_{\rm T}(k) = \lim_{\omega\to 0}\frac{I_{\rm T}(k,\omega)}{E_{\rm T}(k,\omega)} .$$

We note also that the function $\varepsilon'_{\rm T}(k)$ has no physical meaning for $k\neq 0$ at all. This is so because $\lim_{\omega\to 0,k\neq 0}\varepsilon'_{\rm T}(k)/\varepsilon''_{\rm T}(k) = 0$ and the wavevector-dependent conductivity $\sigma_{\rm T}(k) = \frac{{\rm i}\omega}{4\pi}\lim_{\omega\to 0}(\varepsilon_{\rm T}(k,\omega) - 1)$ is determined in terms of the imaginary part $\varepsilon''_{\rm T}(k)$ exclusively.

From the other hand, in the infinite-wavelength limit $k \to 0$ when the conductivity vanishes, $\lim_{k\to 0} \sigma_{\mathrm{T}}(k) = 0$, it is not necessary to consider the real part $\varepsilon'_{\mathrm{T}}(k)$ as an independent quantity because of $\lim_{k\to 0} \varepsilon'_{\mathrm{T}}(k) = \lim_{k\to 0} \epsilon_{\mathrm{T}}(k) = \varepsilon_0$.

The normalized time correlation functions $\Phi_{\mathrm{T}}(k,t) = g_{\mathrm{T}}(k,t)/g_{\mathrm{T}}(k)$ and $\Upsilon(k,t) = s_{\mathrm{T}}(k,t)/s_{\mathrm{T}}(k)$, related to dynamical polarization and magnetization fluctuations, are plotted in figs. 4 and 5, respectively. The librational oscillations superimposed on the exponential, found previously [1, 6] for longitudinal polarization fluctuations, are identified for transverse functions $\Phi_{\mathrm{T}}(k,t)$ as well. But the oscillations damp more quickly and their amplitudes are much smaller in this case. The oscillations vanish completely at larger wavevectors, namely at $k > 20k_{\min}$. The magnetization correlation functions $\Upsilon_{\mathrm{T}}(k,t)$ also exhibit oscillatory features, which are more visible at small wavenumbers. These functions, however, can accept as positive as well as negative values, contrary to the polarization correlations $\Phi_{\mathrm{T}}(k,t)$ which remain positive anywhere in time space. It is worth remarking that after a sufficiently long period, the polarization functions decay purely exponentially in time. This fact has been taken into account by us to calculate the contributions of long tails into the dielectric function $\epsilon_{\mathrm{T}}(k,\omega)$ at time integration (14) of $g_{\mathrm{T}}(k,t)$. In order to demonstrate again that the true choice of microscopic variables $\hat{\boldsymbol{\mathcal{P}}}_{\mathrm{T}}$ and $\hat{\boldsymbol{\mathcal{M}}}_{\mathrm{T}}$ for describing polarization and magnetization fluctuations in ISM fluids is so important, analogous functions, $\langle \hat{\mathscr{P}}_{\mathrm{T}}(\boldsymbol{k},0)\cdot\hat{\mathscr{P}}_{\mathrm{T}}(-\boldsymbol{k},t)\rangle_0 \big/ \langle \hat{\mathscr{P}}_{\mathrm{T}}(\boldsymbol{k},0)\cdot\hat{\mathscr{P}}_{\mathrm{T}}(-\boldsymbol{k},0)\rangle_0$ and $\langle \hat{\mathscr{M}}_{\mathrm{T}}(\boldsymbol{k},0)\cdot\hat{\mathscr{M}}_{\mathrm{T}}(-\boldsymbol{k},t)\rangle_0 \big/ \langle \hat{\mathscr{M}}_{\mathrm{T}}(\boldsymbol{k},0)\cdot\hat{\mathscr{M}}_{\mathrm{T}}(-\boldsymbol{k},0)\rangle_0$, obtained in the PD approximation, are also included in figs. 4 and 5 as dashed curves. The time correlation functions $\Phi_{\mathrm{T}}(k,t)$ and $\Upsilon(k,t)$, corresponding to the exact interaction site description (equations (12) and (13)), are identical to PD functions in the infinite-wavelength limit $k \to 0$, but they differ between themselves in a characteristic way at greater wavevector values, namely, at $k > k_{\min}$.

The real $\epsilon'_{\mathrm{T}}(k,\omega)$ and imaginary $\epsilon''_{\mathrm{T}}(k,\omega)$ parts of the transverse dielectric function $\epsilon_{\mathrm{T}}(k,\omega) = \epsilon'_{\mathrm{T}}(k,\omega) - \mathrm{i}\epsilon''_{\mathrm{T}}(k,\omega)$ for the TIP4P water as depending on frequency at fixed nonzero wavevectors are shown in figs. 6 and 7 as solid and dashed curves, respectively. We mention that $\lim_{k\to 0} \epsilon_{\mathrm{T}}(k,\omega) = \lim_{k\to 0} \varepsilon_{\mathrm{L,T}}(k,\omega) = \varepsilon(\omega)$. For the purpose of comparison the corresponding result obtained previously [1] for the longitudinal dielectric permittivity $\varepsilon_{\mathrm{L}}(k,\omega)$ is also included in fig. 6. The frequency dependence of the transverse dielectric function $\epsilon_{\mathrm{T}}(k,\omega)$ at low enough ω can be described by the Debye theory for arbitrary wavevectors. This is a result of the fact that the polarization correlation functions $g_{\mathrm{T}}(k,t)$ damp exponentially at long times. With increasing frequency the collective molecular

librations take a prominent role in forming the frequency shape for $\epsilon_{\rm T}(k,\omega)$, especially at small and intermediate wavevector values when $k \leq 20k_{\rm min}$. In this wavenumber region, above some $\omega(k)$=1-10 THz corresponding to the position of the first maximum of $\epsilon''_{\rm T}(k,\omega)$, the relaxation behaviour changes into a librational resonance process, characterizing by a frequency of order 100 THz. This frequency is associated with the position of the second maximum of $\epsilon''_{\rm T}(k,\omega)$, which practically does not depend on wavevector. At sufficiently great frequencies the transverse component tends to the longitudinal dielectric constant, so that, for example, at small wavenumbers $k \leq 2k_{\rm min}$ the both components become indistinguishable from one another at $\omega > 10$ THz (see fig. 6). For larger wavevectors the transverse function (fig. 7) differs from the longitudinal one (figs. 6, 7 of [1]) considerably. Beginning from frequencies of order $\omega \sim 1000$ THz and wavevectors of order $k \sim 100\text{Å}^{-1}$ the transverse dielectric function tends to the limiting value $\varepsilon_\infty = 1$ corresponding to nonpolarizable systems.

B. Magnetic properties

The wavevector- and frequency-dependent magnetic susceptibility $\chi(k,\omega) = \mu(k,\omega) - 1 = -\chi'(k,\omega) - {\rm i}\chi''(k,\omega)$ has been evaluated for the TIP4P water using fluctuation formula (16). Its real $\chi'(k,\omega)$ and imaginary $\chi''(k,\omega)$ parts are plotted in fig. 8 as functions of frequency at fixed wavevectors by solid and dashed curves, respectively. We note that fluctuation formula (16) is somewhat other by the structure than fluctuation formulas (2) and (14) for dielectric functions $\varepsilon_{\rm L}(k,\omega)$ and $\epsilon_{\rm T}(k,\omega)$. That is why, unlike the dielectric susceptibility $\epsilon_{\rm L,T}(k,\omega) - 1$, the magnetic susceptibility $\chi(k,\omega)$ vanishes in the static limit at arbitrary wavenumbers, $\lim_{\omega\to 0}\chi(k,\omega) \equiv \chi(k) = 0$, and this statement follows directly from equation (16). From the physical point of view, such a situation is explained by the different nature of electric and magnetic dipoles in ISM fluids. While the electric dipole moment $\boldsymbol{d}_i$ is fixed by the rigid molecular geometry, resulting in $|\boldsymbol{d}_i| = d$ =const, the magnetic moment $\boldsymbol{m}_i$ is caused by the rotational motion of charges sites and it depends explicitly on the angular velocity $\boldsymbol{\Omega}_i$ of the molecule. Thus, the vector $\boldsymbol{m}_i$ varies in time not only due to the orientational dynamics of the molecule, as $\boldsymbol{d}_i$-vector, but also owing to the changes of $\boldsymbol{\Omega}_i$, so that $|\boldsymbol{m}_i| \neq$const. As a result, the macroscopic magnetization does not appear in the presence of static magnetic fields $\boldsymbol{H}_0$, because then $\langle\boldsymbol{\Omega}_i\rangle = 0$ even if the spatial inhomogeneity of $\boldsymbol{H}_0$ is taken into account (quasiequilibrium, stationary state of the system).

At nonzero frequencies, when the system is far from equilibrium ($\langle \boldsymbol{\Omega}_i \rangle \neq 0$) due to the presence of external timely inhomogeneous fields, two mechanisms of appearing the macroscopic magnetization are possible. The first mechanism, is connected with the alignment of own magnetic dipole moments along the field $\boldsymbol{H}_0$, leading to a paramagnetic-like behaviour with $\chi'(k,\omega) > 0$. The second one is caused by the magnetizability of molecules owing to the changes of angular velocities in magnetic fields. Then the corresponding additional magnetic moment of the system will be directed oppositely to $\boldsymbol{H}_0$-vector that may lead to a diamagnetic-like behaviour with $\chi'(k,\omega) < 0$. As we can see from fig. 8, at relatively small frequencies, the TIP4P water exhibits paramagnetic features. Beginning from frequencies of order 100-300 THz (in dependence on wavevector) and higher the diamagnetic contributions into the magnetization become to dominate and the system under consideration behaves like a diamagnetics. It is interesting to remark that the frequencies $\omega_{\rm p}$ and $\omega_{\rm d}$, corresponding to maximal values of $|\chi'(k,\omega)|$ in the paramagnetic and diamagnetic regions, respectively, almost do not depend on wavevector in a wide wavenumber range from $k = 0$ up to $k \leq 20k_{\rm min}$, where they are equal to $\omega_{\rm p} \sim 80$ THz and $\omega_{\rm d} \sim 180$ THz, indicating about a weak influence of the translational motions on the processes of magnetization.

Applying the Laplace boundary theorem to fluctuation formula (16) yields the magnetic susceptibility $\chi_\infty(k) = \lim_{\omega\to\infty} \chi(k,\omega) = -hs_{\rm T}(k) \leq 0$ in the infinite-frequency regime, where $s_{\rm T}(k) = \lim_{t\to 0} s_{\rm T}(k,t) > 0$ is the static autocorrelation function. The function $\chi_\infty(k)$ is plotted in fig. 9 by the solid curve. It takes negative values at arbitrary finite wavenumbers and tends to zero as far as $k \to \infty$ (note that the magnetic susceptibility is shown in figs. 8 and 9 for convenience in the negative representation $-\chi$). The existence of a nonzero coefficient for the magnetic susceptibility in the infinite-frequency regime may be considered as a somewhat unexpected result. For example, the dielectric susceptibilities $\epsilon_{\rm L,T}(k,\omega) - 1$ vanish (as $\sim 1/\omega^2$) at $\omega \to \infty$, because electric dipoles are unsensitive to very fast changes of finite electric fields in time owing to the inertness of molecules. For the case of magnetic susceptibility the pattern is different for the following reason. According to material relations, the macroscopic magnetization of the system can be presented in the form $\boldsymbol{\mathcal{M}}_{\rm T}(\boldsymbol{k},\omega) = \frac{1}{4\pi}\frac{\chi(k,\omega)}{1+\chi(k,\omega)}\boldsymbol{B}_{\rm T}(\boldsymbol{k},\omega)$. The vector of magnetic induction is not independent at $k,\omega \neq 0$ and expressed in terms of the electric field using the Maxwell equation as $\boldsymbol{B}_{\rm T}(\boldsymbol{k},\omega) = -\frac{c}{\omega}\boldsymbol{k}\times\boldsymbol{E}(\boldsymbol{k},\omega)$. So that in the infinite-frequency regime the macroscopic magnetization $\boldsymbol{\mathcal{M}}_{\rm T}(\boldsymbol{k},\omega)$ vanish as $1/\omega$ at finite values of electric fields $\boldsymbol{E}(\boldsymbol{k},\omega)$, despite the fact that $\chi_\infty(k) \neq 0$. A nonvanishing magnetization of the

system can be achieved at $\omega \to \infty$ for infinite values ($\boldsymbol{E}(\boldsymbol{k},\omega) \sim \omega$) of electric fields only. But this corresponds rather a hypothetical case which is hard to realize in practice. Moreover, it cannot be handled within the linear response theory, where the smallness of electromagnetic fields is assumed in advance.

The value of function $\chi_\infty(k)$ in the infinite-wavelength limit can be presented in an analytical form. Acting in the spirit of derivation of analytical formulas for the static current correlations (see Appendix) and taking into account explicit expression (13) for the microscopic magnetization density $\hat{\boldsymbol{\mathcal{M}}}_{\rm T}$, one obtains the following result

$$\chi_\infty = \lim_{k\to 0}\chi_\infty(k) = -\frac{1}{3}\frac{\pi N}{c^2 V}\sum_{a,b}^{M} q_a q_b \sum_{\alpha,\beta}^{X,Y,Z}\left(\left[\frac{1}{J}-\frac{2}{J_\alpha}\right](\Delta_a^\alpha\Delta_b^\beta)^2 + \frac{1}{J_\alpha}\Delta_a^\alpha\Delta_a^\beta\Delta_b^\alpha\Delta_b^\beta\right) \ , \quad (19)$$

where J_α are the moments of inertia of the molecule with respect to its three principal axes X, Y, Z, the αth component of vector-position $\boldsymbol{\delta}_i^a$ for site a in the molecular principal coordinate system is denoted as Δ_a^α and $1/J = 1/J_X + 1/J_Y + 1/J_Z$. It can be shown easily that in the PD approximation the function $\chi_\infty^{\rm PD}(k) = -h\langle\hat{\mathscr{M}}_{\rm T}(\boldsymbol{k},0)\cdot\hat{\mathscr{M}}_{\rm T}(-\boldsymbol{k},0)\rangle_0\big/2Nd^2$ does not depend on wavevector, i.e., $\chi_\infty^{\rm PD}(k) = \chi_\infty$ (the horizontal dashed line in fig. 9). The values of $\chi_\infty^{\rm PD}(k)$ computed in the MD calculations are shown in the figure as open circles. They differ from the exact value χ_∞ within statistical noise. Using equation (19) we obtain for the TIP4P model: $\chi_\infty \approx -6.7\cdot 10^{-10}$ that is too small in comparison with the diamagnetic susceptibility $\chi_{\rm H_2O} \approx -9\cdot 10^{-6}$ of real water. This is so because ISMs do not take into account an electronic subsystem which gives the main contribution into the magnetic susceptibility owing to the smallness of the mass $m_{\rm e}$ of electron. This contribution can be estimated noticing that the diamagnetic susceptibility of an ideal electron gas is defined as $\chi_{\rm e} \sim -Ne^2\langle\rho_{\rm e}^2\rangle\big/Vm_{\rm e}c^2$, where e is the electron charge and $\langle\rho_{\rm e}^2\rangle$ denotes the averaged value of square radius-vectors of electrons within the molecule [24]. Comparing this result with formula (19) and taking into account that $\langle\rho_{\rm e}^2\rangle \sim r^2$, $|q_a| \sim |e|$, $\max_\alpha[1/J_\alpha] \sim 1/m_{\rm H}r^2$ and $\boldsymbol{\Delta}_a{}^2 \sim r^2$ yields $\chi_\infty/\chi_{\rm e} \sim m_{\rm e}/m_{\rm H} \sim 10^{-4} \sim \chi_\infty/\chi_{\rm H_2O}$, where $m_{\rm H}$ is the mass of a hydrogen atom. It is necessary to point out that the atomic diamagnetic susceptibility (19) in the infinite-frequency limit, like the case of electronic diamagnetism, does not depend on temperature of the system and it is determined by the geometry of the molecule. We note that such an atomic diamagnetism can be absent for some particular molecular geometries. For example, for the simplest ξDS model, when $M = 2$, $q_1 = q$, $q_2 = -q$, $\boldsymbol{\Delta}_1 = \boldsymbol{l}$ and $\boldsymbol{\Delta}_2 = -\boldsymbol{l}$, we find from equation (19) that $\chi_\infty^{\xi\rm DS} = 0$.

We would like also to emphasize that fluctuation formula (16), which explicitly involves the microscopic magnetization density, is only the way to calculate the magnetic suscep-

tibility $\chi(k,\omega)$ of ISM fluids in computer experiment not only for nonzero wavevectors but also at $k = 0$. Such a numerical calculation cannot be done within the abbreviated description, despite the fact that according to relation (17), the knowledge of the longitudinal $\varepsilon_{\rm L}(k,\omega)$ and transverse $\varepsilon_{\rm T}(k,\omega)$ components of the generalized dielectric permittivity (equations (2) and (6)) allows one, in principle, to determine the frequency-dependent magnetic susceptibility $\chi(\omega)$ in the infinite-wavelength limit $k \to 0$. The reasons for this situation are following. First of all we underline that relation (17) is valid for nonzero but very small values of wavevector, namely, for $k \lesssim \omega/c$. Even for relatively great frequencies of order 1000 THz this condition corresponds to $k \lesssim 0.0003\text{Å}^{-1}$. At the same time, the smallest nonzero value of wavevectors accessible in our simulations is $k_{\rm min} \sim 0.3\text{Å}^{-1}$. So that to reach the value 0.0003Å^{-1} it is necessary to increase the size of the simulation box to 1000 times! From the other hand, at $k = k_{\rm min}$ we can use relation (17) beginning from a frequency of order $\omega \sim ck_{\rm min} \sim 10^6$ THz, where $\varepsilon_{\rm T}(k_{\rm min},\omega) \approx \chi_\infty(k_{\rm min})$. But it is known in advance that the magnetic susceptibility of the system is too small, consisting, for instance, approximately $-7.5 \cdot 10^{-10}$ for $\chi_\infty(k)$ at $k = k_{\rm min}$. Therefore, to reproduce this value using the difference of functions $\varepsilon_{\rm L}(k_{\rm min},\omega)$ and $\varepsilon_{\rm T}(k_{\rm min},\omega)$ it is required to compute them with a relative statistical accuracy of order 10^{-12} at least that constitutes an unrealistic problem again. For example, even at extra long simulations with 1 000 000 time steps, as in our case, the relative statistical uncertainties for the dielectric quantities are of order 1%, i.e., 10^{-2} only.

C. Propagation of electromagnetic waves

We consider now the question of propagation of free transverse electromagnetic waves, $E(\boldsymbol{r},t) \sim \mathrm{e}^{\mathrm{i}(\omega t - \boldsymbol{k}\cdot\boldsymbol{r})}$, in the TIP4P water. The dispersion relation, connecting frequency and wavenumber of the waves in dielectrics, is of the form [18]:

$$\omega^2 - \frac{c^2k^2}{\varepsilon_{\rm T}(k,\omega)} = 0 \ . \tag{20}$$

In this case $\omega \sim ck$ and, as it follows from equation (15), the transverse functions $\varepsilon_{\rm T}(k,\omega)$ and $\epsilon_{\rm T}(k,\omega)$ differ from one another by order of $\chi(k,\omega)$. As was shown in the preceding subsection, the magnetic susceptibility of ISM systems is sufficiently small at arbitrary wavevectors and frequencies, i.e., $\chi(k,\omega) \ll 1$. Thus we can putt $\varepsilon_{\rm T}(k,\omega) \approx \epsilon_{\rm T}(k,\omega)$ in relation (20) without loss of precision. Further, the characteristic frequency scale of varying the dielectric constant is of order 1000 THz. This corresponds to an interval of

varying wavenumbers in the waves of order 0.0003Å^{-1}. At the same time, the characteristic wavevector scale of varying $\epsilon_{\text{T}}(k,\omega)$ is of order $k_{\min} \sim 0.3\text{Å}^{-1}$, so that the spatial dispersion of the dielectric constant in equation waves (20) can be neglected completely, i.e., $\varepsilon_{\text{T}}(k,\omega) \approx \epsilon_{\text{T}}(k,\omega) \approx \varepsilon(\omega)$. The dielectric permittivity $\varepsilon(\omega)$ is an imaginary function of frequency. Therefore, a solution to the equation (20) with respect to wavenumbers at a given real frequency (it corresponds to frequency of the source which creates electromagnetic waves) it is necessary to find in the form $\boldsymbol{k} = \boldsymbol{k'} - \mathrm{i}\boldsymbol{k''}$, where the magnitude k'' of the imaginary part will describe the damping of waves with the wavelength $\lambda = 2\pi/k'$. We shall consider a case when plane waves are damped in direction of their propagation, i.e., when $\boldsymbol{k'}\cdot\boldsymbol{k''} = k'k''$.

Numerical results for the dispersion $\omega(k')$ and damping $k''(\omega)$, coefficients in the infrared region of spectrum are shown in figs. 10a and 10b, respectively. We note that calculation of the damping coefficient at great frequencies is very sensitive to the precision of evaluation of the dielectric constant. A more accurate estimation can be achieved when the dielectric constant is determined in terms of current fluctuations via fluctuation formula (5) (the solid curve in fig. 10b), instead of the usual formula (2) (the open circles). As far as $k'' \neq 0$ in the whole region of frequencies $0 < \omega < \infty$, purely monochromatic waves cannot propagate in dielectrics. Nevertheless, choosing a criterion $k'' \ll k'$, we can talk about quasimonochromatic waves with a slight absorption. According to our calculation, only two opposite regions of very small ($\omega \lesssim 0.01$ THz; radiowaves) and very great ($\omega \gtrsim 500$ THz; far infrared, visible light) frequencies can satisfy this criterion. In the radiowaves region (see insets of the figures), the phase velocity $\omega(k')/k' = c/\sqrt{\varepsilon_0}$ is defined by the static dielectric constant $\sqrt{\varepsilon_0} \approx 7$ (for real water $\sqrt{\varepsilon_0} \approx 9$). For example, at $\omega \approx 0.01$ THz we obtain $k'c \approx 0.1$ THz and $k''c \approx 0.002$ THz. Thus, the radiowaves with the wavelength $\lambda = 2\pi/k' \approx 2$cm are dumped in a characteristic way during the interval $2\pi/k'' \approx 1$m. In the far infrared region the phase velocity of the nonpolarizable TIP4P water tends to its infinite frequency value $c/\sqrt{\varepsilon_\infty}$, where $\varepsilon_\infty = \lim\limits_{\omega\to\infty} \varepsilon(\omega) = 1$. Owing to the electronic polarizability of molecules, which is not taken into account in the TIP4P model, the dielectric constant of real water differs from unity even in the visible light spectrum $\omega \sim 3000$ THz, where $\sqrt{\varepsilon(\omega)} \approx 1.33$. It is interesting to remark about the existence of a large region of frequencies ($\omega \sim 10 - 50$ THz), where the group velocity $\partial\omega(k')/\partial k' = c/\sqrt{\varepsilon^*}$ is practically constant. In this region, near the librational minimum of the imaginary part $\varepsilon''(\omega)$, the real part $\varepsilon'(\omega)$ of the dielectric constant approximately does not depend on frequency and takes values of order $\varepsilon^* \approx 2.3$ (see fig. 6a of Ref. [1]

for $\varepsilon(\omega)$ and fig. 6a of the present paper for $\epsilon_{\rm T}(k_{\rm min},\omega) \approx \varepsilon(\omega)$). However, the waves are damped significantly ($k'' < k'$) in this frequency range. Within the absorption maximum, which occurs at ~ 150 THz, we have $k'' \sim k'$, so that electromagnetic waves decay here on an interval of order of their wavelengths.

All our previous calculations of the dielectric functions $\varepsilon_{\rm L,T}(k,\omega)$ dealt with real values of wavevector and frequency. Such functions at a given single set of k and ω describe the response of the system on electromagnetic fields in the form of monochromatic plane waves $\sim {\rm e}^{{\rm i}(\omega t - \boldsymbol{k}\cdot\boldsymbol{r})}$. Imaginary values of frequency and wavevector correspond to cases when amplitudes of fields either increase or decrease in time and space. Since arbitrary inhomogeneous fields can be cast as a set of the monochromatic waves, using the time and spatial Fourier transform, the dielectric function at imaginary values of k and ω may be expressed in terms of its values at real wavevectors and frequencies. As a demonstration, we consider the case of purely imaginary frequencies, $\omega \equiv {\rm i}\omega^*$, in the infinite wavelength limit ($k = 0$). Then, as it follows from fluctuation formula (2), the dielectric constant can be calculated directly

$$\frac{\varepsilon(\omega^*) - 1}{\varepsilon_0 - 1} = \left(1 + \omega^* \int\limits_0^\infty {\rm e}^{\omega^* t} \Phi(t) {\rm d}t \right) \ , \tag{21}$$

using the time correlation function $\Phi(t) = \left\langle \sum_{i,j}^N \boldsymbol{d}_i(0)\boldsymbol{\cdot}\boldsymbol{d}_j(t) \right\rangle_0 \Big/ \left\langle \sum_{i,j}^N \boldsymbol{d}_i(0)\boldsymbol{\cdot}\boldsymbol{d}_j(0) \right\rangle_0$ of the total dipole moment. From the other hand, presenting the field $\sim {\rm e}^{-\omega^* t}$ in the form of the corresponding Fourier integral over real frequencies, it can be shown, in particular, that at $\omega^* < 0$ the dielectric constant $\varepsilon(\omega^*)$ is expressed via the imaginary part of $\varepsilon(\omega)$ (defined at real frequencies) as follows [17]:

$$\varepsilon(\omega^*) - 1 = \frac{2}{\pi} \int\limits_0^\infty \frac{x\varepsilon''(x)}{x^2 + \omega^{*2}} {\rm d}x \ . \tag{22}$$

The function $\varepsilon(\omega^*)$ is plotted in fig. 11a. It describes the response of the system on external electric fields which increase in time exponentially. As was expected, this function at $\omega^* \to -\infty$ tends to unity owing the inertness of polar molecules.

The case $\omega^* > 0$ will correspond to decaying in time of electric fields. This decaying can be caused either by decreasing of external fields or by switching off of sources which support these fields. As an example, consider the spatial and time decay of electromagnetic fields in the system after the passage of transverse electromagnetic waves. In this situation, frequency and wavevector are purely imaginary quantities, i.e., $\omega \equiv {\rm i}\omega^*$ with $\omega^* > 0$ and $k \equiv -{\rm i}k''$, that is necessary to take into account finding a solution to the equation

(20). For the same reasons as in the case of propagation of electromagnetic waves, we put $\varepsilon_{\rm T}(k,\omega) \approx \varepsilon(\omega)$ in equation (20) and obtain $\omega^* = ck''/\sqrt{\varepsilon(\omega^*)}$, where $\varepsilon(\omega^*)$ accepts purely real values at purely imaginary frequencies. We note that an independent parameter in this equality is k'', so that the function $\omega^*(k'')$ will describe the time decay $\sim {\rm e}^{-\omega^* t}$ of the transverse electric field with a spatial inhomogeneity of k'' which has been created by the passed electromagnetic wave (see fig. 10b). The function $\omega^*(k'')$ is shown in fig. 11b. As can be seen, weak spatial inhomogeneities correspond to long life times $\sim 1/\omega^*(k'')$, whereas strong inhomogeneous fields damp in time faster. It is worth to remark also that in the asymptotic limit $t \to \infty$, the time correlation function $\Phi(t)$ decays in time exponentially as $\sim {\rm e}^{-t/\tau_{\rm rel}}$, where $\tau_{\rm rel} = 6.7$ps is the relaxation time. Therefore, the dielectric constant $\varepsilon(\omega)$ at imaginary frequencies can be defined only in the region $\Im\omega < 1/\tau_{\rm rel} = 0.149$ THz, because otherwise the integral in (21) is divergent. This merely means that transverse electromagnetic excitations cannot damp in time faster than with the characteristic interval $\tau_{\rm rel}$. The limiting region of imaginary frequencies is shown in fig. 11b by the horizontal dashed line.

Finally, as far as real $\varepsilon'_{\rm T}$ and imaginary $\varepsilon''_{\rm T}$ parts of the transverse wavevector- and frequency-dependent dielectric constant are defined according to the fluctuation formula (6) via the same time correlation function $c_{\rm T}(k,t)$, they are not independent and must be connected between themselves. The desired relations can be obtained using analytical properties of the functions $c_{\rm T}(k,t)$, $\varepsilon'_{\rm T}(k,\omega)$ and $\varepsilon''_{\rm T}(k,\omega) - 4\pi\sigma_{\rm T}(k)/\omega$. The result is

$$\varepsilon'_{\rm T}(k,\omega) - 1 = \frac{2}{\pi} \int\limits_0^\infty \frac{x\varepsilon''_{\rm T}(k,x)}{x^2-\omega^2}{\rm d}x \ , \qquad \varepsilon''_{\rm T}(k,\omega) = -\frac{2\omega}{\pi} \int\limits_0^\infty \frac{\varepsilon'_{\rm T}(k,x)-1}{x^2-\omega^2}{\rm d}x + \frac{4\pi\sigma_{\rm T}(k)}{\omega} \ . \tag{23}$$

The relations (23) are similar to the well-known Kramers-Kronig expressions for the dielectric constant of conductors [17]. They can be applied to the transverse frequency-dependent dielectric constant of ISMs at arbitrary values of wavevector.

IV. CONCLUSION

We have established that the calculation of the dielectric quantities for interaction site models of polar fluids can be performed in computer experiment by two alternative ways, namely, using either charge or current fluctuations. The first way is more efficient to evaluate the longitudinal component $\varepsilon_{\rm L}(k,\omega)$ of the dielectric permittivity, whereas

the second method is suitable to obtain its transverse part $\varepsilon_{\rm T}(k,\omega)$. Separating the total current of moving charges into electrical and magnetic components, the transverse generalized dielectric permittivity $\varepsilon_{\rm T}(k,\omega) = \epsilon_{\rm T}(k,\omega) + \frac{c^2k^2}{\omega^2}\frac{\chi(k,\omega)}{1+\chi(k,\omega)}$ has been expressed in terms of the transverse dielectric $\epsilon_{\rm T}(k,\omega)$ and magnetic $\chi(k,\omega)$ functions. These functions have been evaluated for the TIP4P model of water by molecular dynamics simulations in the whole region of wavevectors and frequencies for the first time on the basis of the proposed fluctuation formulas.

It has been shown that the transverse $\epsilon_{\rm T}(k,\omega)$ and longitudinal $\epsilon_{\rm L}(k,\omega) \equiv \varepsilon_{\rm L}(k,\omega)$ components of the dielectric tensor $\boldsymbol{\epsilon}(\boldsymbol{k},\omega)$ differ between themselves in a characteristic way and coincide with one another in opposite limits of either very small wavenumbers or very large wavevector and frequency values. Moreover, contrary to the case of longitudinal fluctuations, the generalized dielectric permittivity $\varepsilon_{\rm T}(k,\omega)$ exhibits a specific behaviour when both wavenumber and frequency tend to zero. We has identified also that at great frequencies the TIP4P water can be considered as a weak diamagnetics. However, values of the magnetic susceptibility $\chi(k,\omega)$ are much smaller in amplitude than those for real water, because the electronic magnetization is not included in this model. It is worth to stress that in the present investigation the polarization and magnetization microscopic densities have been constructed taking into account explicitly the atomic structure of ISMs. As a result, it has been demonstrated, in particular, that at nonzero wavevectors the genuine transverse dielectric function $\epsilon_{\rm T}(k,\omega)$ has nothing to do with that obtained in the point dipole approximation. The last function behaves like the dielectric permittivity of a Stockmayer system [12–14] and can be used at small wavenumbers only as an estimation of the frequency-dependent dielectric constant in the infinite-wavelength limit.

The longitudinal and transverse components of the wavevector- and frequency-dependent dielectric permittivity describe all electromagnetic phenomena in the system. The knowledge of these quantities may present an interest in both theory and pure experiment. The performed calculations can be extended, in principle, to more realistic models of polar fluids. This will be the subject of a separate consideration.

The author would like to acknowledge financial support by the President of Ukraine.

Appendix

We shall show that the longitudinal and transverse components $c_{\rm L,T}(k)$ of the static wavevector-depended Kirkwood factor of second order $c(k) = c_{\rm L}(k) + 2c_{\rm T}(k)$ are presented analytically. According to definitions (3) and (7), the functions $c(k)$ and $c_{\rm L}(k)$ read

$$
\begin{aligned}
c(k) &= \frac{1}{Nd^2} \left\langle \sum_{i,a}^{N,M} q_a \boldsymbol{V}_i^a \cdot \sum_{j,b}^{N,M} q_b \boldsymbol{V}_j^b \, \mathrm{e}^{-\mathrm{i}\boldsymbol{k}\cdot(\boldsymbol{r}_i^a - \boldsymbol{r}_j^b)} \right\rangle_0 \ , \\
c_{\rm L}(k) &= \frac{1}{Nd^2} \left\langle \sum_{i,a}^{N,M} q_a (\hat{\boldsymbol{k}}\cdot\boldsymbol{V}_i^a) \sum_{j,b}^{N,M} q_b (\hat{\boldsymbol{k}}\cdot\boldsymbol{V}_j^b) \, \mathrm{e}^{-\mathrm{i}\boldsymbol{k}\cdot(\boldsymbol{r}_i^a - \boldsymbol{r}_j^b)} \right\rangle_0 \ ,
\end{aligned}
\tag{A1}
$$

where the site velocities can be split as $\boldsymbol{V}_i^a = \boldsymbol{V}_i + \boldsymbol{\Omega}_i \times \boldsymbol{\delta}_i^a$. We mention that $\boldsymbol{V}_i$ and $\boldsymbol{\Omega}_i$ are the translational and angular velocities of the ith molecule, respectively, $\boldsymbol{\delta}_i^a = \boldsymbol{r}_i^a - \boldsymbol{r}_i$ and $\boldsymbol{r}_i$ denotes the position of the molecular centre of mass.

Equilibrium distribution functions are factored into the coordinate and velocity parts. In its turn, translational and angular velocities are distributed independently of one another for each molecule. As a result, nonzero contributions to equilibrium averaging give only terms with coincident molecular indexes ($i = j$) of summation (A1). It is more convenient to consider each molecule in its own principal coordinate system in which $\boldsymbol{\delta}_i^a \equiv \boldsymbol{\Delta}_a$. Then expressions (A1) transform into

$$
\begin{aligned}
c(k) &= \frac{1}{Nd^2} \sum_{i}^{N} \sum_{a,b}^{M} q_a q_b \left\langle \left(\boldsymbol{V}_i^2 + [\boldsymbol{\Omega_i}\times\boldsymbol{\Delta}_a]\cdot[\boldsymbol{\Omega_i}\times\boldsymbol{\Delta}_b] \right) \mathrm{e}^{-\mathrm{i}\boldsymbol{k}\cdot\boldsymbol{\rho}_{ab}} \right\rangle_0 \ , \\
c_{\rm L}(k) &= \frac{1}{Nd^2} \sum_{i}^{N} \sum_{a,b}^{M} q_a q_b \left\langle \left((\hat{\boldsymbol{k}}\cdot\boldsymbol{V}_i)^2 + (\hat{\boldsymbol{k}}\cdot[\boldsymbol{\Omega_i}\times\boldsymbol{\Delta}_a])(\hat{\boldsymbol{k}}\cdot[\boldsymbol{\Omega_i}\times\boldsymbol{\Delta}_b]) \right) \mathrm{e}^{-\mathrm{i}\boldsymbol{k}\cdot\boldsymbol{\rho}_{ab}} \right\rangle_0 \ ,
\end{aligned}
\tag{A2}
$$

where $\boldsymbol{\rho}_{ab} = \boldsymbol{\Delta}_a - \boldsymbol{\Delta}_b$. It is necessary to underline that for a given molecular geometry, $\boldsymbol{\Delta}_a$ ($a = 1, \ldots, M$) constitute the set of constant vectors characterizing the positions of charged sites in the principal coordinate system attached to the molecule. Further, we use the following equalities $3(\hat{\boldsymbol{k}}\cdot[\boldsymbol{\Omega}\times\boldsymbol{\Delta}_a])(\hat{\boldsymbol{k}}\cdot[\boldsymbol{\Omega}\times\boldsymbol{\Delta}_b]) = (3\hat{\boldsymbol{k}}\hat{\boldsymbol{k}} - \mathbf{1}) : \boldsymbol{\Omega}\times\boldsymbol{\Delta}_a\boldsymbol{\Omega}\times\boldsymbol{\Delta}_b + [\boldsymbol{\Omega}\times\boldsymbol{\Delta}_a]\cdot[\boldsymbol{\Omega}\times\boldsymbol{\Delta}_b]$ and $[\boldsymbol{\Omega}\times\boldsymbol{\Delta}_a]\cdot[\boldsymbol{\Omega}\times\boldsymbol{\Delta}_b] = \Omega^2(\boldsymbol{\Delta}_a\cdot\boldsymbol{\Delta}_b) - (\boldsymbol{\Omega}\cdot\boldsymbol{\Delta}_a)(\boldsymbol{\Omega}\cdot\boldsymbol{\Delta}_b)$ and take into account the relations

$$
\left\langle \mathrm{e}^{-\mathrm{i}\boldsymbol{k}\cdot\boldsymbol{\rho}} \right\rangle_{\hat{\boldsymbol{k}}} = j_0(k\rho) \ , \qquad \left\langle (3\hat{\boldsymbol{k}}\hat{\boldsymbol{k}} - \mathbf{1}) \mathrm{e}^{-\mathrm{i}\boldsymbol{k}\cdot\boldsymbol{\rho}} \right\rangle_{\hat{\boldsymbol{k}}} = -j_2(k\rho)(3\hat{\boldsymbol{\rho}}\hat{\boldsymbol{\rho}} - \mathbf{1}) \ ,
\tag{A3}
$$

where $j_0(z) = \sin(z)/z$, $j_2(z) = 3j_1(z)/z - j_0(z)$ are the spherical Bessel functions of order zero and two, respectively, $\hat{\boldsymbol{\rho}} = \boldsymbol{\rho}/\rho$ and averaging in (A3) is performed over orientations of $\hat{\boldsymbol{k}}$-vector with respect to the molecule. Owing identity of molecules and isotropy of the system we have, in particular, $\langle V_i^2 \rangle = \langle V^2 \rangle$, $\langle \Omega_i^2 \rangle = \langle \Omega^2 \rangle$ and $\langle (\hat{\boldsymbol{k}}\cdot\boldsymbol{V})^2 \rangle = \langle V^2 \rangle / 3$. Using the definition

of temperature and the equipartition theorem yields $m\langle V^2\rangle_0/3 = J_\alpha\langle\Omega_\alpha^2\rangle_0 = k_{\rm B}T$, where m is the mass of the molecule and Ω_α are the principal components ($\alpha = X, Y, Z$) of angular velocity. Finally, in view of the statistical independence of angular velocities directed along different principal axes of inertia, after cumbersome but not complicate operations one obtains

$$c(k) = \frac{k_{\rm B}T}{d^2}\sum_{a,b}^{M} q_a q_b j_0(k\rho_{ab})\left[\frac{3}{m} + \sum_{\alpha}\left(\frac{1}{J} - \frac{1}{J_\alpha}\right)\Delta_a^\alpha\Delta_b^\alpha\right], \tag{A4}$$

$$\begin{aligned} c_{\rm L}(k) &= \frac{1}{3}c(k) - \frac{k_{\rm B}T}{3d^2}\sum_{a\neq b}^{M} q_a q_b j_2(k\rho_{ab})\sum_{\alpha,\beta} h_{ab}^{\alpha\beta}\left(3\hat\rho_{ab}^\alpha\hat\rho_{ab}^\beta - \delta_{\alpha\beta}\right), \\ c_{\rm T}(k) &= \frac{c(k) - c_{\rm L}(k)}{2} = \frac{1}{3}c(k) + \frac{k_{\rm B}T}{6d^2}\sum_{a\neq b}^{M} q_a q_b j_2(k\rho_{ab})\sum_{\alpha,\beta} h_{ab}^{\alpha\beta}\left(3\hat\rho_{ab}^\alpha\hat\rho_{ab}^\beta - \delta_{\alpha\beta}\right), \end{aligned} \tag{A5}$$

where $h_{ab}^{\alpha\beta} = -\Delta_a^\beta\Delta_b^\alpha/J_\gamma$ and $h_{ab}^{\alpha\alpha} = \Delta_a^\beta\Delta_b^\beta/J_\gamma + \Delta_a^\gamma\Delta_b^\gamma/J_\beta$ (all the three variables α, β and γ take different values here) denote the constant quantities which are defined by the molecular geometry and ρ_{ab} is the distance between sites a and b within the same molecule.

Thus, the static Kirkwood factor of second order is uniquely determined by the temperature and geometry of molecules. It is the same for infinite and finite systems, i.e, $C_{\rm L,T}(k) = c_{\rm L,T}(k)$ (infiniteness of the system has not been used at the derivation of equations (A4) and (A5)). As can been shown earlier, this statement is completely in line with transformations (9).

REFERENCES

[1] Omelyan, I.P., 1998, *Molec. Phys.*, **93**, 123.

[2] Bopp, P.A., Kornyshev A.A., and Sutmann G., 1996, *Phys. Rev. Lett.*, **76**, 1280.

[3] Omelyan, I.P., 1996, *Phys. Lett. A*, **223**, 295.

[4] Impey, R.W., Madden, P.A., and McDonald, I.R., 1982, *Molec. Phys.*, **46**, 513.

[5] Edwards, D.M.F., Madden, P.A., and McDonald, I.R., 1984, *Molec. Phys.*, **51**, 1141.

[6] Neumann, M., 1986, *J. Chem. Phys.*, **85**, 1567.

[7] Anderson, J., Ullo, J.J., and Yip, S., 1987, *J. Chem. Phys.*, **87**, 1726.

[8] Fonseca, T., and Ladanyi, B.M., 1990, *J. Chem. Phys.*, **93**, 8148.

[9] Skaf M.S., Fonseca T., and Ladanyi B.M., 1993, *J. Chem. Phys.*, **98**, 8929.

[10] Skaf M.S., and Ladanyi B.M., 1995, *J. Chem. Phys.*, **102**, 6542.

[11] Ladanyi B.M., and Skaf M.S., 1996, *J. Phys. Chem.*, **100**, 1368.

[12] Omelyan, I.P., 1996, *Phys. Lett. A*, **220**, 167.

[13] Neumann, M., 1986, *Molec. Phys.*, **57**, 97.

[14] Omelyan, I.P., 1996, *Molec. Phys.*, **87**, 1273.

[15] Raineri, F.O., Resat, H., and Friedman, H.L., 1992, *J. Chem. Phys.*, **96**, 3068.

[16] Raineri, F.O., and Friedman, H.L., 1993, *J. Chem. Phys.*, **98**, 8910.

[17] Landau, L.D., and Lifshitz E.M., 1984, *Electrodynamics of Continuous Media* (Oxford: Pergamon).

[18] Bredov, M.M., Rumyantsev V.V., and Toptigin I.N., 1985, *Classical Electrodynamics* (Moscow: Nauka) [in Russian].

[19] Bertolini, D., and Tani, A., 1992, *Molec. Phys.*, **75**, 1047.

[20] Bertolini, D., and Tani, A., 1992, *Molec. Phys.*, **75**, 1065.

[21] Jorgensen, W.L., Chandrasekhar, J., Madura, J.D., Impey, R.W. and Klein, M.L., 1983, *J. Chem. Phys.*, **79**, 926.

[22] Omelyan, I.P., 1997, *Comput. Phys. Commun.*, **107**, 113.

[23] Omelyan, I.P., 1998, *Comput. Phys. Commun.*, **109**, 171.

[24] Terletski Ya.P., Rubakov Yu.P., 1990, *Electrodynamics* (Moscow: Vusshaya shkola) [in Russian].

Figure captions

Fig. 1. The wavevector-dependent longitudinal Kirkwood factor $g_{\rm L}(k)$ **(a)** and the longitudinal and transverse components $c_{\rm L,T}(k)$ **(b)** of the current autocorrelation function for the TIP4P water. The dashed and solid curves in **(a)** correspond to the finite and infinite systems in the ISRF geometry. The results of the Ewald geometry for the longitudinal and transverse components are presented by the full squares and circles, respectively, whereas the corresponding data in **(b)** obtained within the ISRF geometry are displayed as open squares and circles. The analytical evaluation of $c_{\rm L,T}(k)$ (equation (A5)) is plotted in **(b)** by the solid curves. The calculations of $g_{\rm L}(k)$, performed through the dynamical current correlations (see equation (8)), are shown by the direct and rotated crosses for the Ewald and ISRF geometries, respectively.

Fig. 2. The normalized dynamical total current correlation functions of the TIP4P water. The result of the Ewald geometry for the longitudinal and transverse components is presented as open and full circles, respectively. The data, obtained within the ISRF geometry for the infinite system, are plotted by the corresponding solid curves. The longitudinal component of the finite system within the ISRF geometry is shown as the dashed curve.

Fig. 3. The wavevector-dependent transverse dielectric function $\epsilon_{\rm T}(k)$ **(a)** and generalized conductivity $\sigma_{\rm T}(k)$ **(b)** in the low frequency limit (the solid curves). The dielectric function corresponding to the PD approximation and the conductivity, calculated in terms of total current (instead of magnetization) correlations are shown in subsets **(a)** and **(b)** as the dashed curve and open circles, respectively.

Fig. 4. The normalized, time autocorrelation functions of the transverse polarization fluctuations in the TIP4P water. The results of the PD approximation are shown as dashed curves. Note that in the infinite-wavelength limit $k \to 0$ (see subset **(a)**), the PD functions are identical to genuine ones.

Fig. 5. The normalized, time autocorrelation functions of the transverse magnetization fluctuations in the TIP4P water. Notations as for fig. 4.

Fig. 6. The transverse component of the wavevector- and frequency-dependent dielectric function $\epsilon_{\rm T}(k,\omega)$ of the TIP4P water at small wavenumbers. The real and imaginary parts are plotted by the bold solid and dashed curves, respectively. For comparison the longitudinal component is shown by the corresponding thin solid and dashed curves.

Fig. 7. The transverse component of the wavevector- and frequency-dependent dielectric function of the TIP4P water at great wavenumbers. The real and imaginary parts are plotted by the solid and dashed curves, respectively.

Fig. 8. The wavevector- and frequency-dependent magnetic susceptibility of the TIP4P water. The real and imaginary parts are plotted by the solid and dashed curves, respectively. Note that the results are shown in a negative representation.

Fig. 9. The wavevector-dependent magnetic susceptibility in the infinite-frequency regime (full circles connected by the solid curve). Note that the result in the PD approximation is independent on wavenumbers (horizontal dashed curve). The PD function calculated in the MD simulations is shown as open circles.

Fig. 10. The dispersion **(a)** and spatial damping **(b)** of transverse electromagnetic waves in the TIP4P water.

Fig. 11. (a) The dielectric constant of the TIP4P water in the infinite-wavelength limit as a function of purely imaginary frequencies. **(b)** The time decay of electromagnetic fields in the system after the passage of transverse electromagnetic waves.

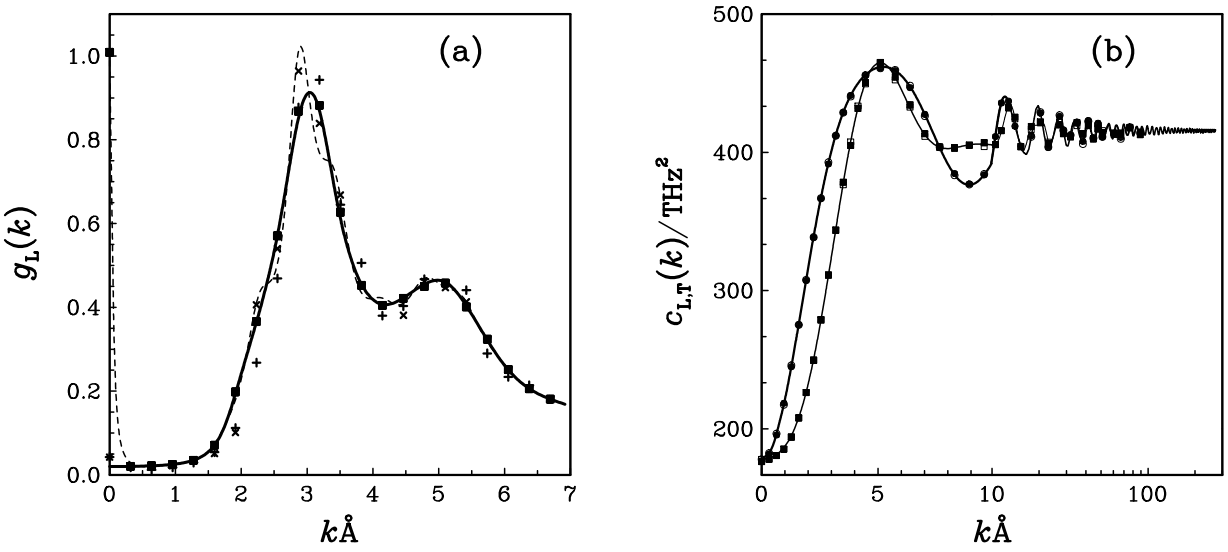
(a)
$g_L(k)$
1.0
0.8
0.6
0.4
0.2
0.0
0
1
2
3
4
5
6
7
kÅ
(b)
$c_{L,T}(k)/\mathrm{THz}^2$
500
400
300
200
0
5
10
100
kÅ

Fig. 1

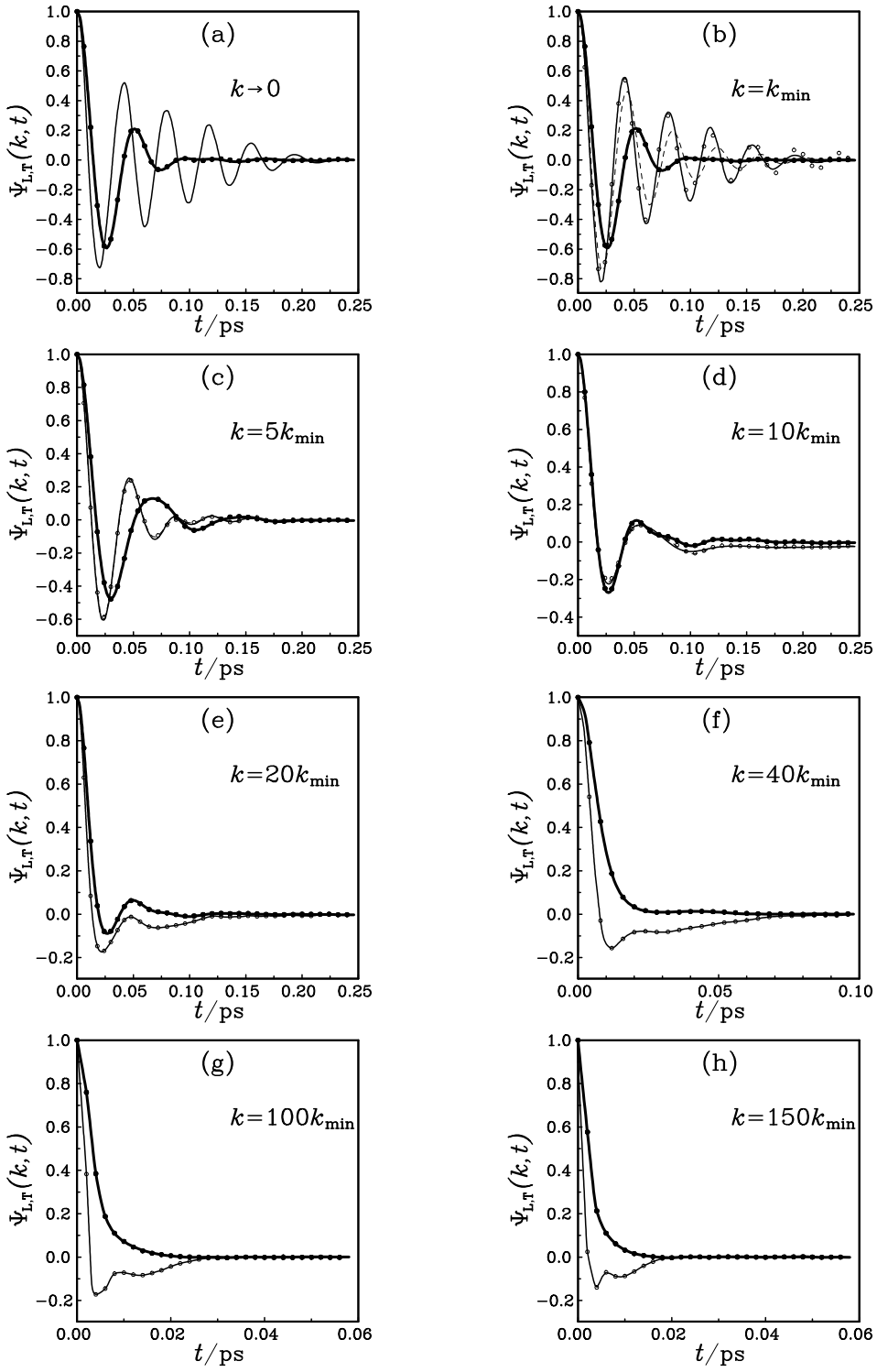
(a)
$k \to 0$
(b)
$k = k_{\min}$
(c)
$k = 5k_{\min}$
(d)
$k = 10k_{\min}$
(e)
$k = 20k_{\min}$
(f)
$k = 40k_{\min}$
(g)
$k = 100k_{\min}$
(h)
$k = 150k_{\min}$
$\Psi_{L,T}(k,t)$
t/ps

Fig. 2

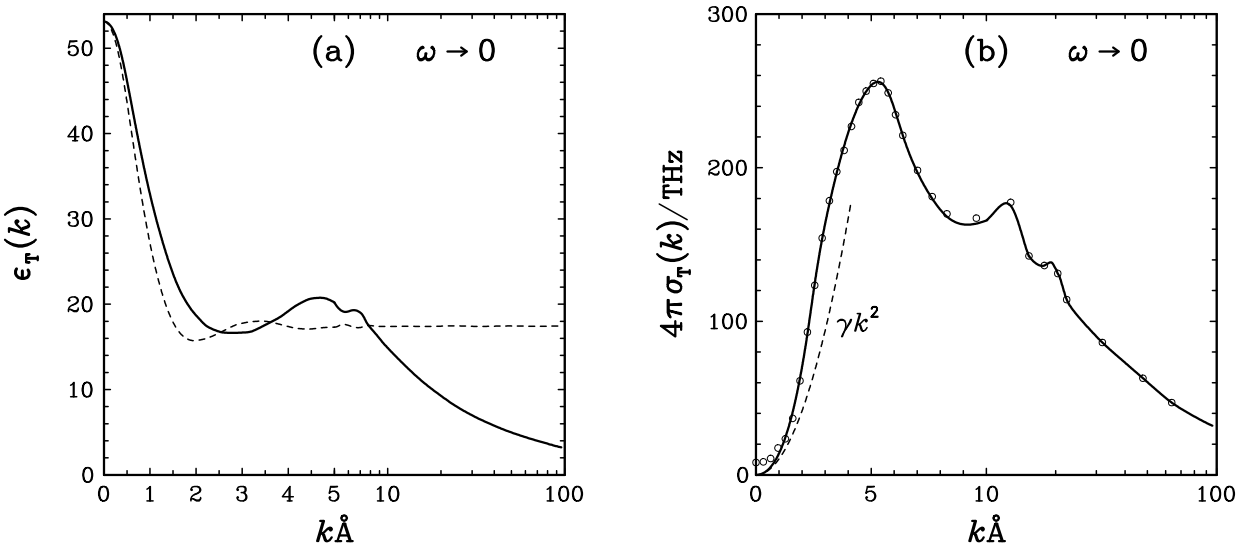

Fig. 3

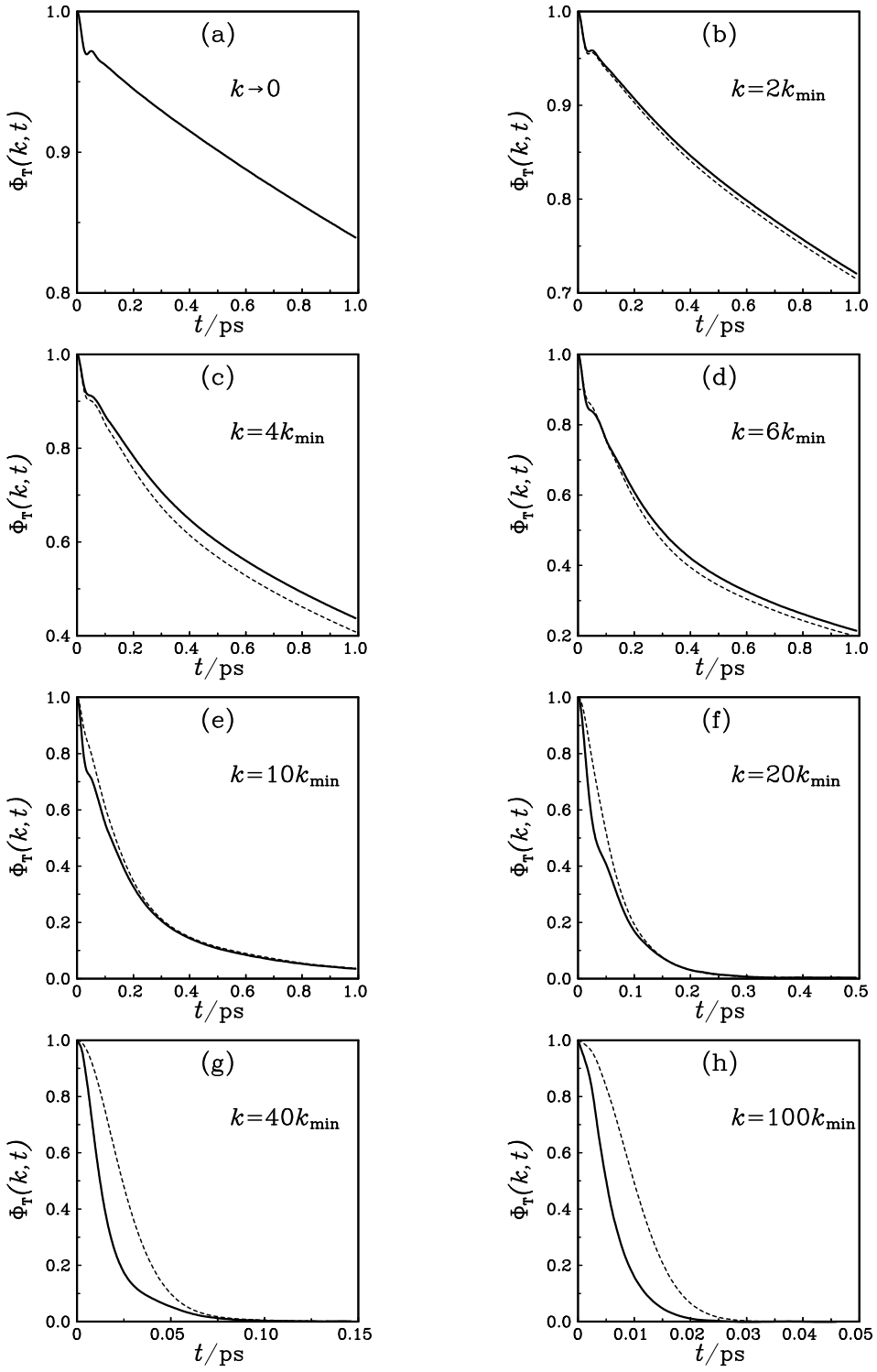
(a)
$k \to 0$
(b)
$k=2k_{\min}$
(c)
$k=4k_{\min}$
(d)
$k=6k_{\min}$
(e)
$k=10k_{\min}$
(f)
$k=20k_{\min}$
(g)
$k=40k_{\min}$
(h)
$k=100k_{\min}$
$\Phi_T(k,t)$
t/ps

Fig. 4

This figure "tfigmdw5.gif" is available in "gif" format from:

http://arXiv.org/ps/physics/9901048v1

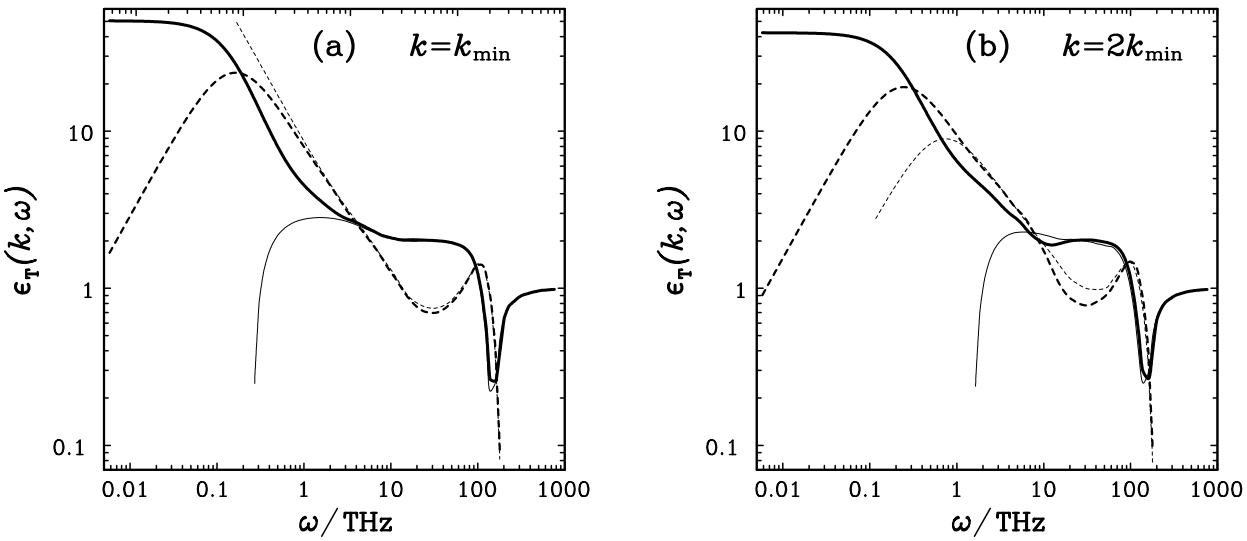
(a) $k=k_{\min}$
(b) $k=2k_{\min}$
$\epsilon_T(k,\omega)$
10
1
0.1
0.01
0.1
1
10
100
1000
$\omega/$ THz

Fig. 6

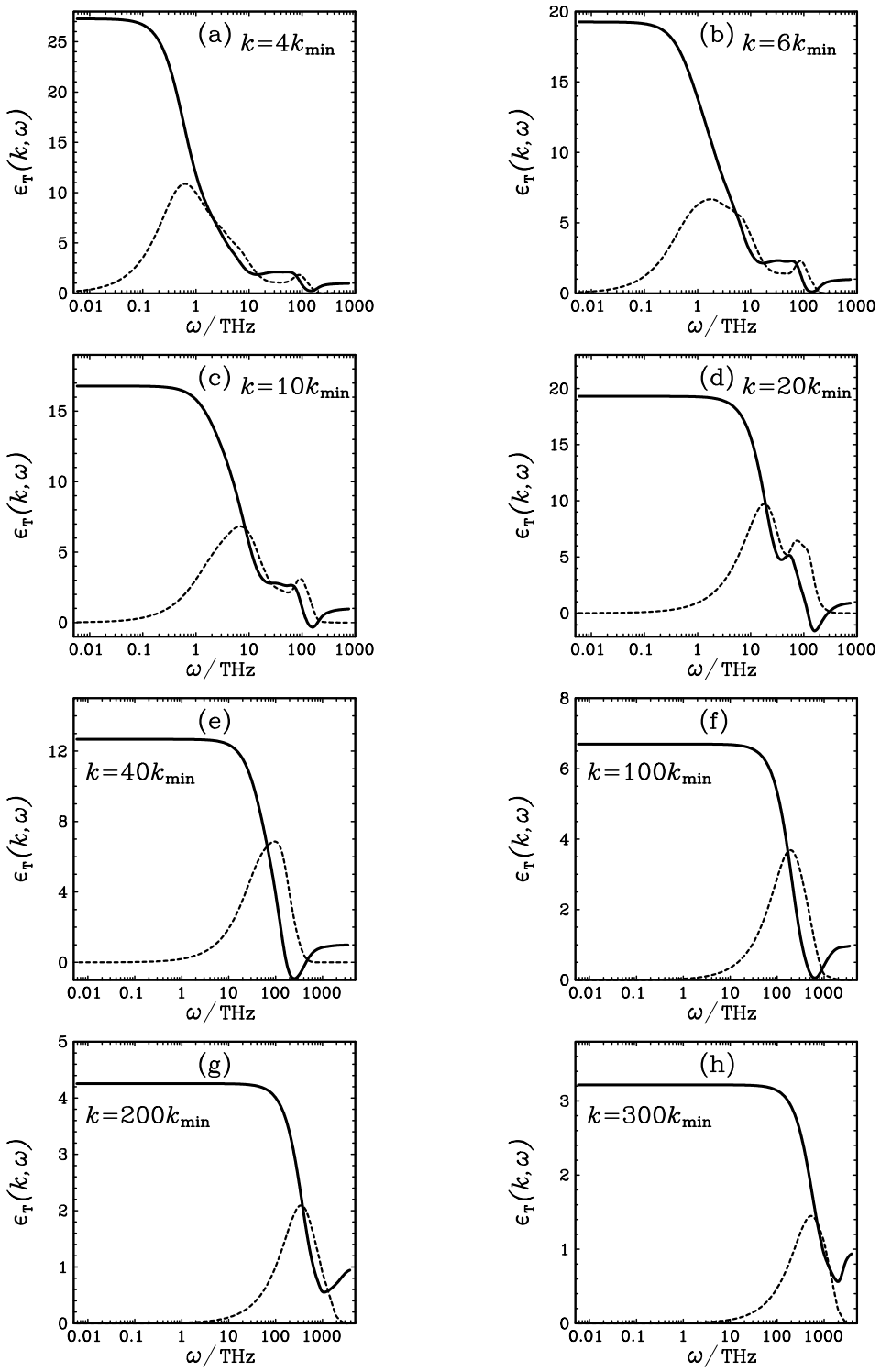
(a) $k=4k_{\min}$
(b) $k=6k_{\min}$
(c) $k=10k_{\min}$
(d) $k=20k_{\min}$
(e) $k=40k_{\min}$
(f) $k=100k_{\min}$
(g) $k=200k_{\min}$
(h) $k=300k_{\min}$
$\epsilon_T(k,\omega)$
ω/THz
0.01 0.1 1 10 100 1000

Fig. 7

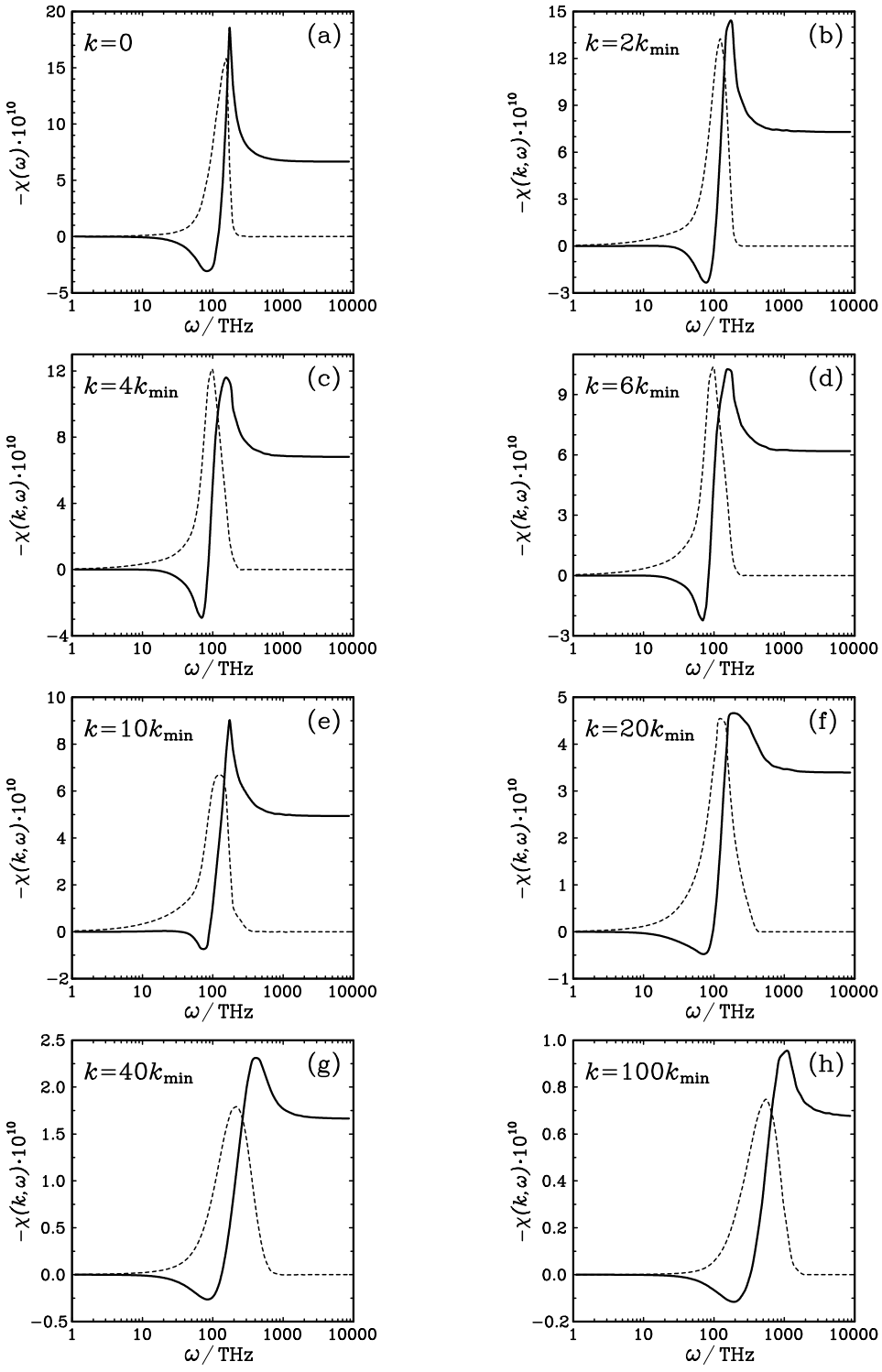
k=0
(a)
k=2k_min
(b)
k=4k_min
(c)
k=6k_min
(d)
k=10k_min
(e)
k=20k_min
(f)
k=40k_min
(g)
k=100k_min
(h)
−χ(ω)·10^10
−χ(k,ω)·10^10
ω / THz

Fig. 8

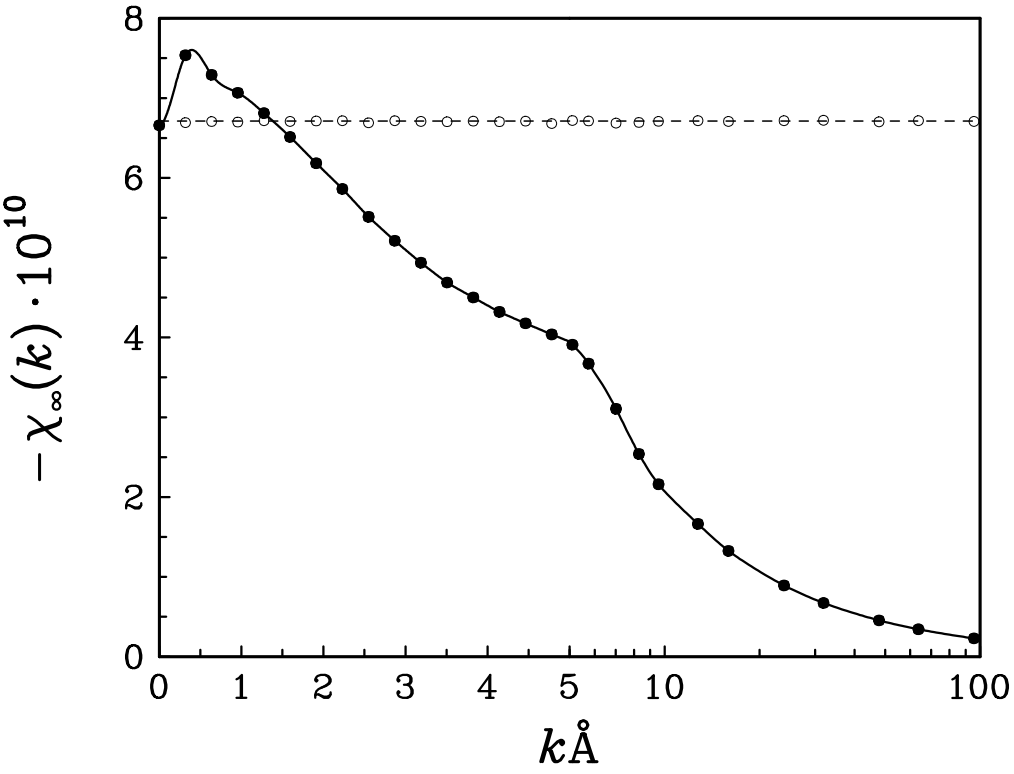

Fig. 9

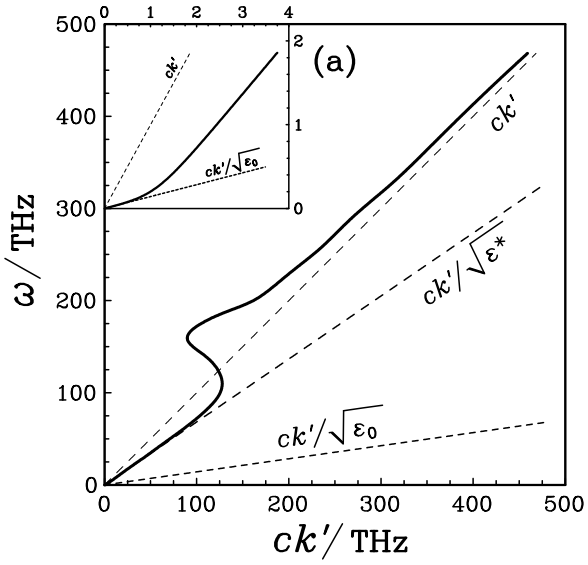
(a)
ω / THz
ck′ / THz
ck′
ck′/√ε*
ck′/√ε0
0
100
200
300
400
500
1
2
3
4

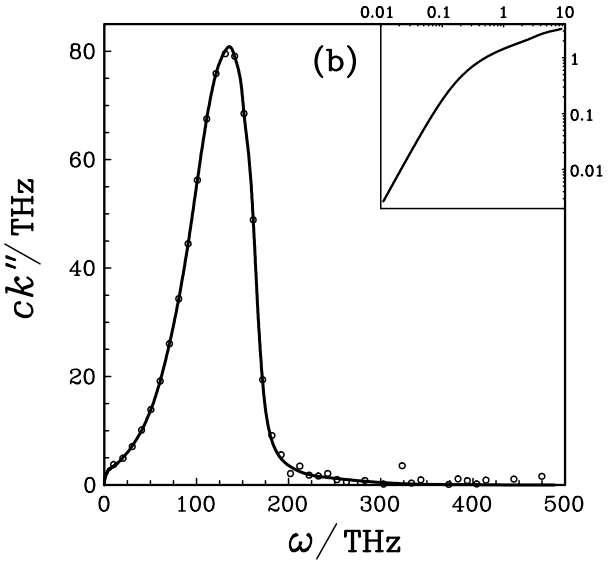
(b)
ck″ / THz
ω / THz
0
20
40
60
80
100
200
300
400
500
0.01
0.1
1
10

Fig. 10

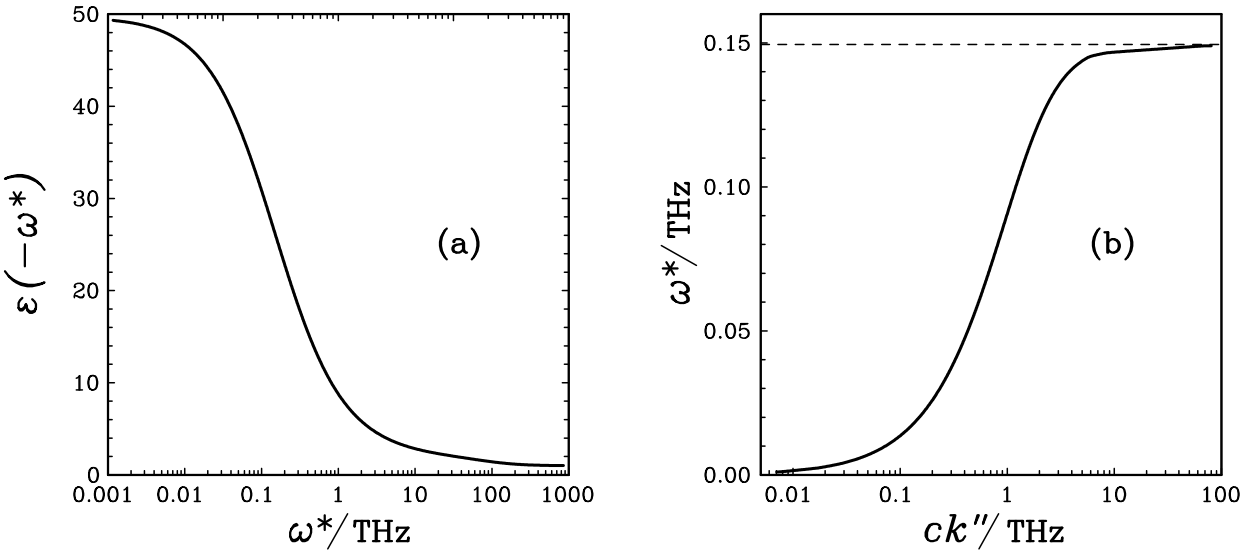
50
40
30
20
10
0
0.001
0.01
0.1
1
10
100
1000
ε(−ω*)
ω*/THz
(a)
0.15
0.10
0.05
0.00
0.01
0.1
1
10
100
ω*/THz
ck″/THz
(b)

Fig. 11